A ROTATING ELECTRODE SYSTEM

FOR THE GENERATION OF METAL ALLOY MICROSPHERES

A Thesis

by

CHAD ALAN THOMPSON

Submitted to the Office of Graduate Studies of
Texas A&M University
in partial fulfillment of the requirements for the degree of

MASTER OF SCIENCE

Approved by:

Chair of Committee,	Sean M. McDeavitt
Committee Members,	Lin Shao
	Haiyan Wang
Head of Department,	Yassin A. Hassan

December 2012

Major Subject: Nuclear Engineering

ABSTRACT

TerraPower LLC is designing a fast breed and burn reactor intended to operate for up to 40 years without refueling, designated as the Travelling Wave Reactor (TWR). Various U-Zr alloy fuel designs have been proposed for the TWR that may require a powder feed for fabrication. A simple and economic option for laboratory scale powder production is the Rotating Electrode Process (REP), which produces microsphere shaped powder by melting the tip of a rotating bar with an electric arc. In order to fully characterize this process for various U-Zr alloys and provide the feed material for testing fabrication techniques, a Rotating Electrode System (RES) was designed and built.

The RES is largely based on a combination of two designs; an early REP system developed by Starmet Corporation in the 19xxa and a later design optimized for U-Mo powder production by Idaho National Laboratory (INL). The RES designed for this work was improved based on input from vendors specializing in their respective areas of expertise and is capable of atomizing up to a 1.26 cm diameter metal alloy rod at 40,000 RPM. Every component of the machine can be disassembled and transferred through a 35.56 cm (14 in) diameter air lock of a glovebox so that it can operate in a controlled environment.

The RES was tested by atomizing various diameter copper rods to prove system functionality. The tests were carried out in air using an argon cover gas in the powder collection chamber, known as the catch pan to limit oxidation rates of the newly generated microspheres. The powder produced showed strong sphericity ranging from

50 μm to 500 μm in diameter. Problems and areas of concern that were encountered during operation have been addressed so that the RES can be further optimized to better atomize U-Zr alloys once transferred into the glovebox.

DEDICATION

This thesis is dedicated to my Grandmother, Mother, and Aunt Susie for teaching me that the grace of God often comes wrapped in adversity. Like you three, I will always do my best to respond to that grace in a manner pleasing to God.

ACKNOWLEDGEMENTS

I would first like to acknowledge Troy and the personal that work in the NUEN machine shop. Many parts of the RES needed to be custom made or altered and I couldn't have done it without their help and recommendations. Next, I would like to acknowledge Curtis Clark at INL for clarifying some technical aspects of the INL fuel atomizer, which made the design process for the RES much easier. Next, I would like to acknowledge both the undergraduate and graduate workers in the FCML for their recommendations, help gathering parts, recording videos, and companionship in those long hours spent in the lab. Finally, I would like to acknowledge Dr. McDeavitt for guiding me with such patience through the entire graduate process. Thank you all so much.

NOMENCLATURE

EBR-II	Experimental Breeder Reactor II
FCML	Fuel Cycle and Materials Laboratory
FIMA	Fissions per Initial Metal Atom
INL	Idaho National Laboratory
LMFBR	Liquid Metal Fast Breeder Reactor
PREP	Plasma Rotating Electrode Process
REP	Rotating Electrode Process
RES	Rotating Electrode System
TWR	Traveling Wave Reactor
VFD	Variable Frequency Drive

TABLE OF CONTENTS

LIST OF FIGURES

LIST OF TABLES

1. INTRODUCTION

The Traveling Wave Reactor (TWR) is a fast breed and burn reactor currently being developed by Terrapower LLC [1]. The reactor is similar to a Liquid Metal Fast Breeder Reactor (LMFBR) but based on a concept first proposed by Saveli Feinberg in 1958. The distinguishing characteristic of the TWR design is the goal to achieve a core lifetime of up to 60 years without refueling; a challenge that incurs many specialized nuclear fuel issues due to very high fuel burnup [2].

Conventional fast breeder reactors use some form of enriched uranium fuel to breed plutonium into a blanket of depleted uranium surrounding the active core. Once the desired amount of plutonium has been produced in the surrounding blanket region, it is removed and reprocessed to recover the remaining uranium and plutonium for new fuel fabrication. Once the active core can no longer sustain criticality, it too will be removed and reprocessed.

Similar to conventional fast breeder reactors, the TWR will use starter fuel that contains enriched uranium to breed plutonium into a surrounding blanket of depleted uranium. However, unlike conventional fast breeder reactors, this process continues until enough plutonium has been bred into the blanket such that the starter fuel can be removed and the reactor can continue operation by shuffling the blanket assemblies into the location of the starter assemblies. If the core is large enough so that there is an abundance of blanket uranium, this process can theoretically continue for decades. After

the core has reached the end of its life, the fuel could undergo a form of melt refining process and be reused as starter fuel for another TWR.

From a fuel performance perspective, the primary challenges with the TWR fuel cycle are related to the very long lifetime of the fuel in a harsh reactor environment. Due to the necessities of the breed and burn system, it has been calculated that fuel would need to achieve approximately 20% Fissions per Initial Metal Atom (FIMA) burnup [2]. This is well beyond the burnup currently achieved by any commercial reactor in the world. However, there has been an experimental fuel type that has successfully achieved this.

The Experimental Breeder Reactor-II (EBR-II) is the only reactor to successfully achieve fuel burnups of up to 20% FIMA using a U-10Zr alloy fuel coupled with HT-9 martensitic steel cladding [3]. As such, this fuel type and cladding combination is currently being considered as a suitable fuel choice for the TWR. Although the final design of the fuel has not been fully determined, it will likely use some form of U-Zr powder as a feed material for fuel fabrication due to the relatively complex fuel shapes that have been theorized which allow for a low smear density.

A low smear density is needed to delay and alleviate issues that arise when the fuel makes contact with the inner wall of the cladding tube as it swells from irradiation. The cladding tube is weakened by eutectics formed with the fuel and diffusive fission products while the internal pressure is increased as the fuel swells. This undesirable combination will cause the cladding tube to rupture and limits the burnup of the fuel. By decreasing the smear density of the fuel, it can swell into itself rather than directly into

the cladding tube. This will not only help delay eutectics from forming but reduces the internal pressure of the cladding tube for much longer if the plume is large enough to accommodate or release the thermal bonding agent. These fuel ingots may be easier to fabricate using a uranium alloy powder rather than using bulk uranium metal.

The first step in characterizing these potential new fuel designs is to fabricate the U-Zr alloy powder. Compared to the various known methods to produce U-Zr powder, the Rotating Electrode Process (REP) is a simple economic option for laboratory scale production. The fundamental application of the REP is to melt the tip of a pre-alloyed U-Zr rod while rotating it at high RPM. As the tip of the rod begins to melt, centrifugal forces will overcome the surface tension of the molten alloy and droplets will be propelled radially where they will re-solidify into spheres prior to hitting the catch pan. This has been demonstrated with pure uranium by the Starmet Corporation as well as with U-Mo alloys by Idaho National Laboratory (INL).

Unfortunately, there is not a complete characterization of U-Zr powder production using the REP; the laboratory scale fuel atomizer found at INL only initiated the process for some uranium alloys [4]. As such, the design and assembly of the Rotating Electrode System (RES) is the focus of this thesis. It will be designed based on the original REP by Starmet Corporation, and another optimized for U-7Mo powder production by INL [5]. Once assembled and tested, it will be optimized and the complete characterization of U-xZr powder production via REP can occur using the RES.

2. BACKGROUND

The history and formulation to the RES is summarized in this chapter. Section 2.1 introduces some of the foundational concepts from powder metallurgy that are relevant to the system. Section 2.2 summarizes some common methods for metal powder production. Section 2.3 provides more detailed background information regarding previous rotating electrode systems and methods employed to produce metallic powder.

2.1 Powder Metallurgy

Powder metallurgy is a relatively broad category of methods for metalworking that typically involves the processing of finely divided metal powder with a characteristic length of less than 1000 μm to fabricate strong, high performance products in an economic manner. Powder processing methods determine the shape, properties, and structure of the final product and are one of the most diverse manufacturing approaches among the metalworking technologies. Many of the processing methods typically involve shaping or compacting the powder and subsequent thermal bonding of the microspheres by sintering [6].

One of the earliest modern powder metallurgy examples can be traced back to William Coolidge who used a tungsten metal powder to fabricate a durable filament for Thomas Edison [6]. The variety of powder metallurgical applications has since grown drastically. Examples include the manufacturing of bearings, automotive transmission gears, armor piercing projectiles, electrical contacts, aircraft brake pads, jet engine

components, and nuclear fuel elements. Powder metallurgy is still a growing field of technology due to its economic advantage, the ability to custom-design unique microstructures, shapes, or properties, and "captive" reasons (i.e. no other viable fabrication method is available) [6].

The economic advantage of powder metallurgy over conventional casting methods arises because of the ability to produce complex shapes in near final form. Other advantages include the absence of higher temperatures and containment methods necessary for molten metal casting. For example, when fabricating gears for the automobile industry, sintered steel powders are used rather than machining every notch out of a block of steel. This significantly trims the production time, waste, and cost [6].

The second reason noted above that powder metallurgy is used is that many products require a unique microstructure or property only possible when fabricating from a powder. A good example of this is U-10Zr nuclear fuel with a smear density of 75%. Casted U-10Zr has a density of ~15.8 g/cc, but in order to get a smear density of 75%, the U-Zr will need to be at 11.85 g/cc [7]. If the U-10Zr is first made into a powder, it can be sintered at the correct packing factor to achieve this smear density.

The third and final reason powder metallurgy is used (i.e., the "captive" reason) is because there is no other viable method to fabricate the product. These products usually consist of materials that are difficult to process, such as reactive and refractory metals [6]. An example is evident in the manufacturing of zirconium metals. Zirconium has a very high affinity for oxygen, which creates a protective film around the surface of the metal. However, it is also very reactive in its molten state and can interact with

conventional ceramic crucibles [8]. Rather than containing molten reactive metal with heavy contamination, zirconium powder may be created and then pressed and sintered at a much lower temperature.

A summary of these reasons to utilize powder metallurgy techniques is presented in Fig. 2-1. This figure uses a Venn diagram to show the three primary reasons for powder metallurgy. The ideal applications for powder metallurgy are in the concept space where two or all of these reasons overlap.

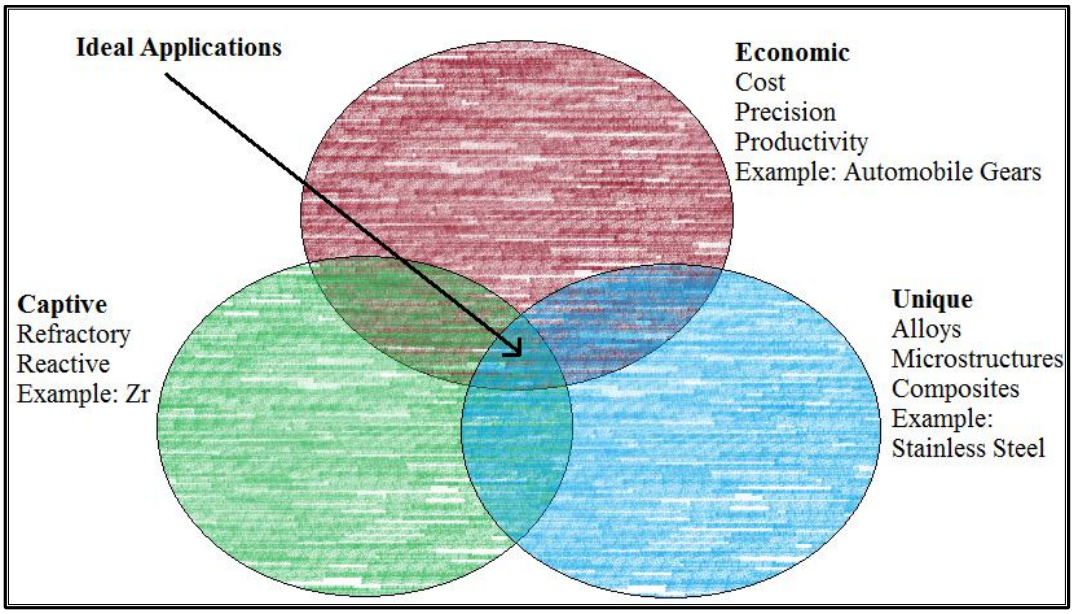

Figure 2-1: Venn diagram for reasons to use powder metallurgy [6].

2.2 Production of Metal Powder

This section will describe four common methods for producing powder: 1) mechanical comminution (Section 2.2.1), 2) chemical reactions (Section 2.2.2), 3)

electrolytic deposition (Section 2.2.3), and 4) liquid metal atomization (Section 2.2.4) to fabricate powder [6]. A specific method may be selected based on the required powder properties needed to fabricate the final product (e.g. size and shape).

2.2.1 Mechanical Comminution

Fabricating powder by mechanical comminution simply means using force to break a material into smaller fragments. The powder formed is usually coarse and irregular in shape. Common methods include impaction, attrition, shearing, or compression of the material until it is the desired size. Multiple methods are often combined in a sequence for effective processing.

The impaction method is usually coupled with the attrition (i.e. rubbing) method in a milling machine. A material is first placed in a cylindrical container with tough, spherical impacting balls. The container is then rotated and the impacting balls collide and rub with the material. The material eventually breaks apart, forming a coarse powder. This method only works well with brittle materials and often contaminates the powder with fine grinding constituents from the impacting ball material and container walls. Figure 2-2 illustrates this concept [6].

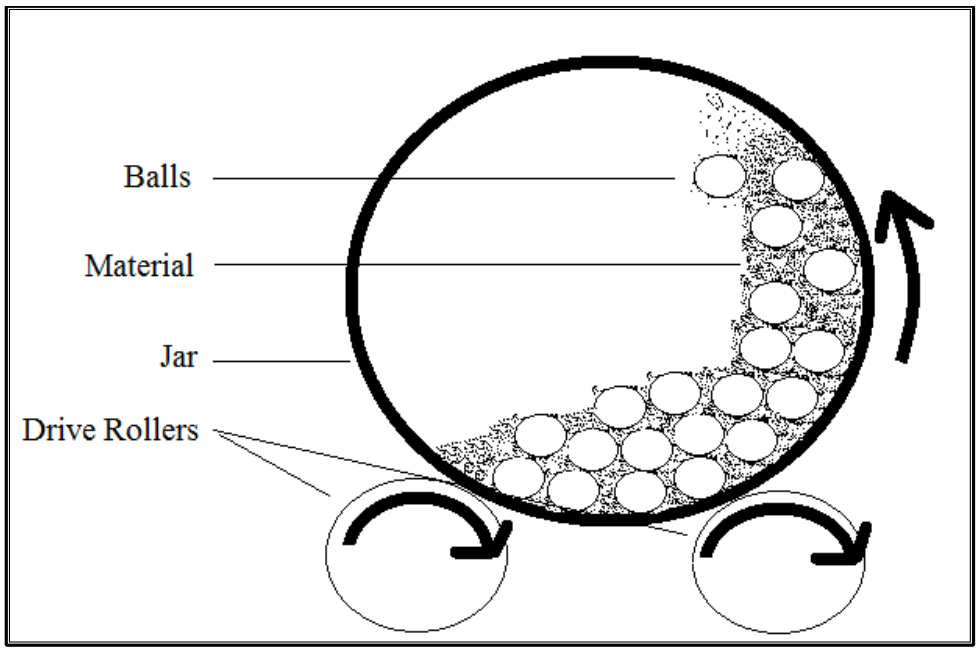

Figure 2-2: Schematic diagram of a rotating milling apparatus

Shearing is usually carried out using a machining tool (e.g., a lathe machine). The material is cut using a bit and the scrap is considered powder. The scrap is usually too irregular in shape and coarse to be useful, and further milling is needed. For this reason, producing powder through shearing is seldom the first choice in powder fabrication [6].

Compaction is the simplest of all the mechanical comminution techniques. It is simply applying enough strain to a brittle material that it breaks apart and is similar to the impaction method. A simple example is squeezing a brittle ceramic. Like the impaction method, the compaction method only works with brittle materials, and forms coarse irregular shaped particles [6].

2.2.2 Chemical Reactions

Nearly all metal powders are formed using solid, liquid, or vapor phase reactions. The size and shape of the powder product can be controlled by varying the reaction variables. Common methods include the decomposition of a solid with a gas, thermal decomposition, precipitation of a liquid, precipitation from a gas, and solid-solid reactive synthesis [6].

Decomposing a solid using a reactive gas is a method more commonly known as oxide reduction. The process starts with an oxide which is milled into a coarse powder, and reduced by a thermochemical reaction using a reducing agent such a hydrogen or carbon monoxide. A volume change occurs as the oxide is reduced, so is taken when designing such a process. The size and shape of the powder can be controlled with gas composition, temperature, and reaction kinetics (i.e. time). Generally, the particles exhibit poor flow and packing characteristics [6].

The thermal decomposition method relies on vapor decomposition and subsequent condensation. A carrier gas reacts with the bulk material that is being fabricated into a powder and gas molecules are formed. This usually requires the reaction chamber to be heated under a vacuum. The gas is then cooled until it condenses and the metal molecule, now in a liquid form, is purified using fractional distillation. The liquid is then reheated with a catalyst to undergo vapor decomposition, which will remove the carrier gas. The gas is then cooled until the metal nucleates out of the gas and is left in a powder form [6].

Precipitating of a solid from a liquid is a method that begins by dissolving the metal into a salt. The salt is then dissolved in water and the metal is precipitated out using a second compound. This works well with reactive and refractory metals such as zirconium and titanium. The precipitated powder is usually on the order of 1 to 10 micrometers in size and can be adjusted by the operating parameters of the salt bath. The powder is typically ~99.5% pure with a few impurities from the salt bath. Powder formed using this method has poor flow and low packing densities [6].

Precipitating a metal powder from a gas is similar to thermal decomposition in which a material is reacted with a carrier gas to form gaseous molecules. The metal is then vapor distilled and nucleated into solid form using an electron beam, laser, or induction field. The product is often sponge like, but powder can be produced down to the nanometer scale. This method is expensive, but the size and shape can be controlled by how the metal is nucleated out of the gas [6].

Fabricating powder using solid state synthesis involves mixing powders of different constituents of an alloy, adding heat, and forming intermetallic compounds. This method is used to form intermetallic compounds of greater thermodynamic stability than the individual constituents. Pure metal powders must be fabricated first, and the alloys formed are restricted to the stoichiometric ratio of the intermetallic compounds. When heat is added to the bed the self-propagating reaction is ignited. The heat must be extracted at the correct rate to prevent melting. The product is a porous structure that can be milled into final dimensions [6].

2.2.3 Atomization

Atomization techniques are commonly used because of their ability to control the size and chemistry of the powder product. Atomization involves the formation of metal microspheres, or coarse powder, from a molten spray. Both pure and alloy metals can be used, and the size of the powder is easily controlled. Common atomization methods are gas, water, and centrifugal atomization.

Gas atomization uses air, nitrogen, helium, or argon jets impinging on a molten stream of metal to form tiny droplets. These droplets are propelled into the collection chamber and will solidify during flight. The whole process is in a large container, which is filled with an inert cover gas to limit or prevent oxidation of the powder. Figure 2-3 illustrates the gas atomization process [6].

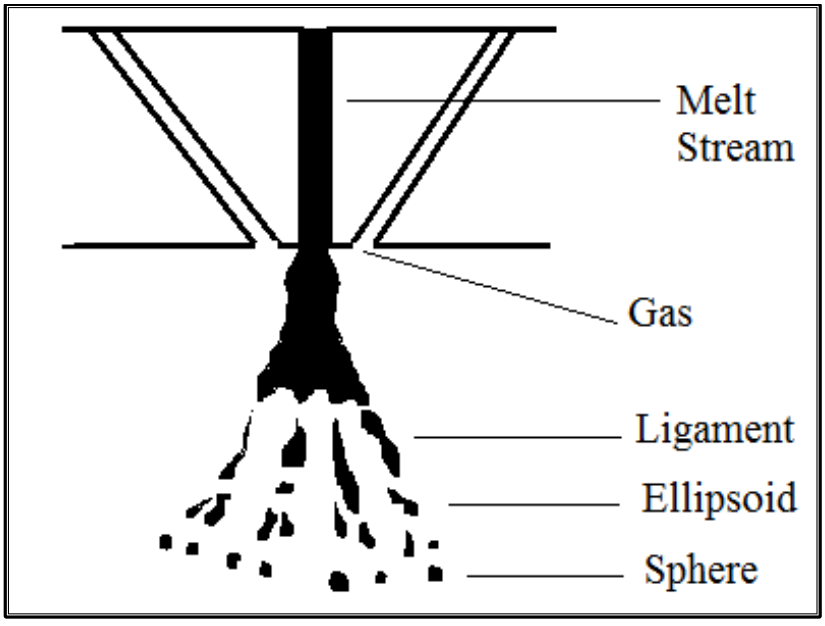

Figure 2-3: The formation of metal powder via gas atomization [6].

The powder morphology may be controlled by operating parameters such as melt temperature, gas type, gas velocity, gas temperature, nozzle design, and metal feed rate. The powder is typically spherical in shape with good packing and flow properties. Nickel-based super-alloys use this technique to produce powder. An example of a simple gas atomizer is depicted in Fig. 2-4 [6].

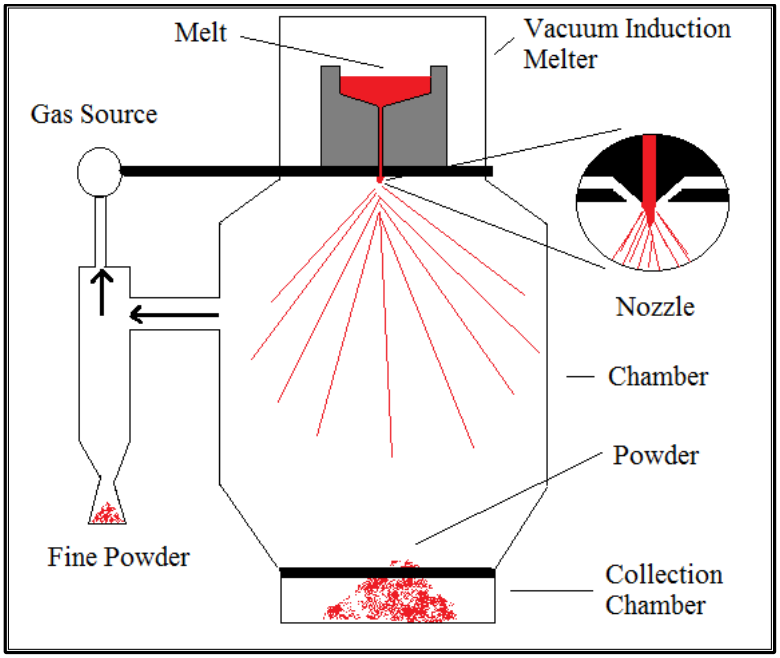

Figure 2-4: A vertical gas atomizer [6].

Water atomization is similar to gas atomization except it uses an impinging jet of water on a molten stream of metal rather than a gas. It is the most common atomization technique for producing elemental and alloyed powders that can be melted below 1600°C. The water allows for rapid quenching to control of the microstructure, but oxidation and irregular shapes often affect the quality of the product. Synthetic oils are

often used in place of water to prevent oxidation. An example of a simple water atomizer is shown in Fig. 2-5 [6].

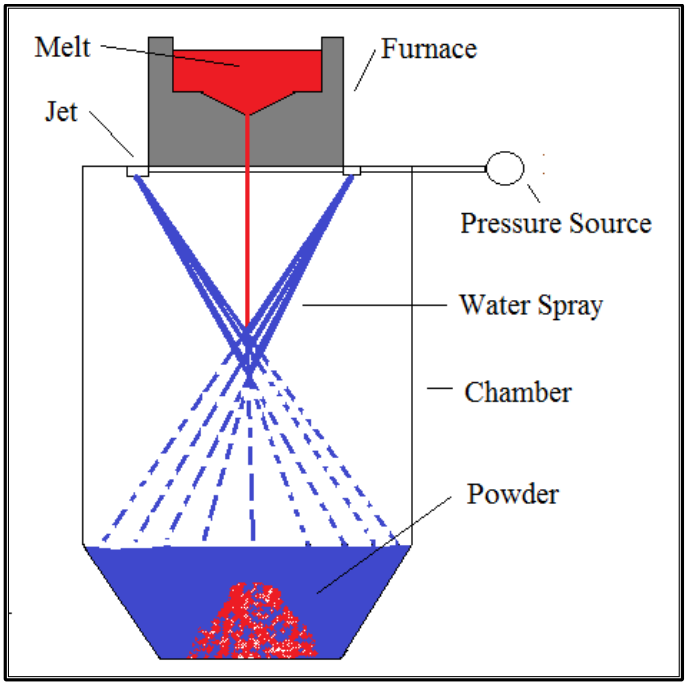

Figure 2-5: A simple diagram of a water atomizer [6].

In the water atomization method, the water or oil pressure is the main control variable for determining powder size. The higher the pressure, the smaller the powder formed. The powder size is on the order of 1 to 10 micrometers and is slightly larger than the powder produced via gas atomization. A common example that uses this technique is stainless steel powder production.

Centrifugal atomization, which is the central topic of this thesis and described more fully in Section 2.3, is a commonly used method for forming reactive and/or

refractory metal powders since other atomization techniques require the metal to be superheated prior to atomization. Figure 2-6 illustrates a rotating electrode process [6]. This method allows for more control over the size distribution than the previous atomization techniques. The metal is fabricated into a cylindrical rod which is then rotated at a high RPM. The tip of the bar is melted and centrifugal forces propel molten droplets radially. The molten spray will then solidify in flight and be collected in a chamber housing the entire process.

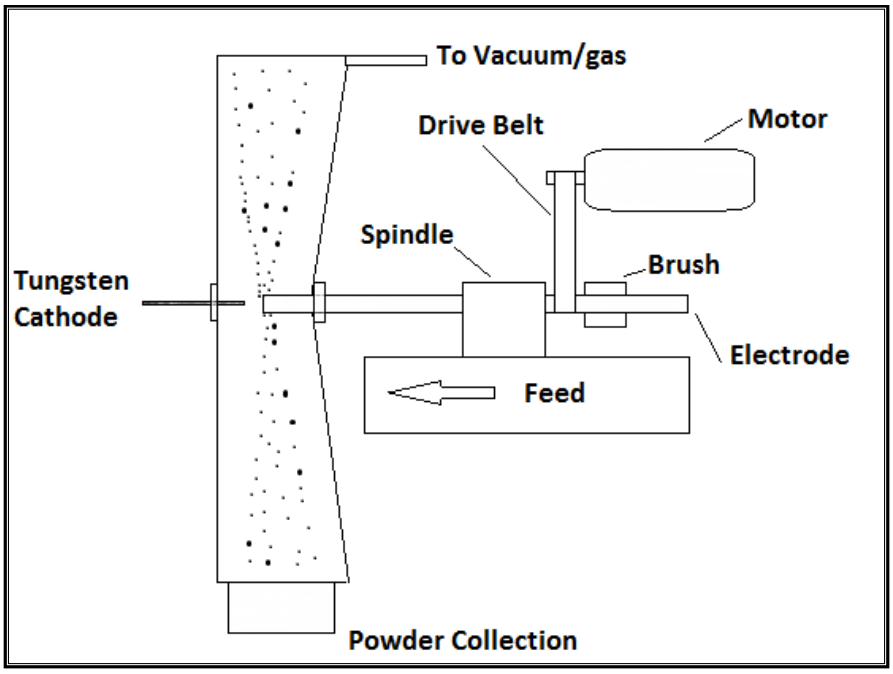

Figure 2-6: Centrifugal atomization by the rotating electrode process [6].

The powder is nearly free of contamination since it uses a contactless form of melting, and very spherical in shape. The powder is nearly uniform in size, ranging from 50 to 1000 micrometers, depending on the RPM used for fabrication. The disadvantages

are a low production rate and if a tungsten cathode is used in the rotating electrode process, there will be some tungsten contamination. Plasma melting is often used to eliminate tungsten contamination [6].

2.2.4 Electrolytic

Electrolytic techniques precipitate a powder at the cathode of an electrolytic cell. The metal that is being fabricated into a powder functions as an anode when placed in an electrolyte with the cathode. When voltage is applied, material at the anode is transferred through the electrolyte and is deposited on the cathode. A sponge-like, very pure precipitate forms on the cathode and can then be dried and milled down into powder. Figure 2-7 illustrates this concept for copper or iron powder production [6]. Electrolytic methods can only be used for the production of elemental metal powders and is rarely preferred due to the higher costs compared to other powder production techniques [6].

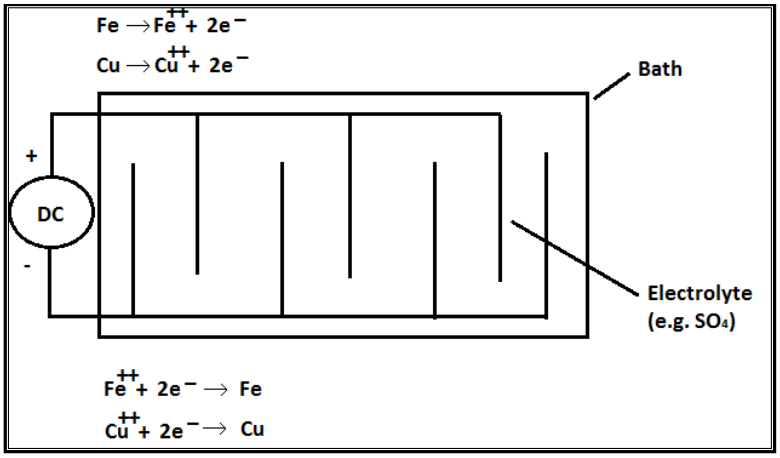

Figure 2-7: Electrolytic cell technique for producing elemental copper or iron powders [6].

2.3 The Rotating Electrode Process

2.3.1 Introduction

The REP is a centrifugal atomization process developed by Starmet Corporation (then Nuclear Metals Inc.) and granted US patents in 1972 [8]. The process consists of melting a metal bar (element or alloy) using an electrical arc or plasma, termed REP/PREP respectively, while it is being rotated along its longitudinal axis at a high RPM. The moment the tip begins to melt, centrifugal forces will propel molten droplets radially as seen in Fig. 2-8 [8]. The propelled molten droplets solidify into microspheres prior to hitting the outer container encapsulating the process. Figure 2-6 illustrates the complete rotating electrode process [8].

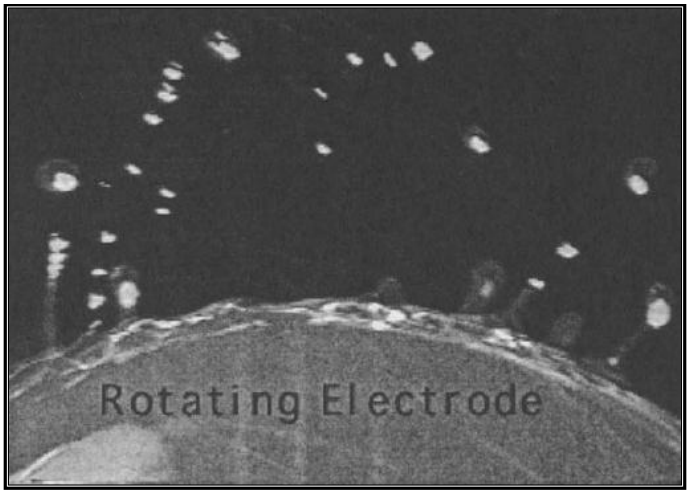

Figure 2-8: Photograph of the rotating electrode process during operation [8].

The REP has several inherent characteristics that make it a suitable choice for producing metal powder. First, it is a contactless form of melting so there is little

contamination in the powder produced; an important characteristic for reactive metals such as zirconium and uranium. Second, the powder produced is almost perfectly spherical, as seen in Fig. 2-9 [8]. This allows for favorable flow properties and a packing density of up to 65%. Thirdly, the size distribution of the powder produced is fairly tight, and the microspheres produced are relatively larger than those produced via gas atomization. Finally, the powder produced is nearly porosity free since it uses centrifugal forces to propel the molten material into droplets rather than aerodynamic drag as used in other atomization techniques [8].

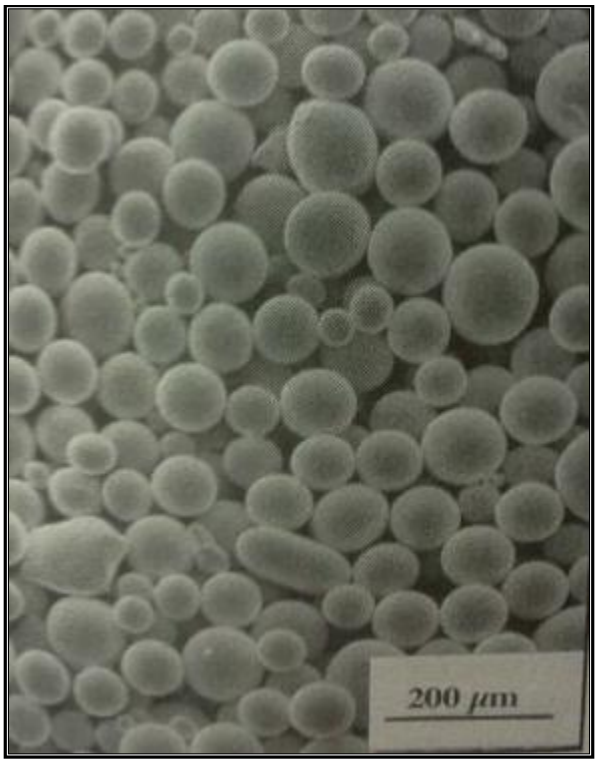

Figure 2-9: Steel powder formed using the rotating electrode process [6].

2.3.2 The Original Design by Starmet Corporation

The original REP design by Starmet, depicted in Fig. 2-10, is a belt-driven system that feeds a rotating metal rod (up to 18,000 RPM) into the proximity of a tungsten electrode as it is melted by an arc established between the two. Mechanical limitations of the bearings and imbalances of the electrode being atomized limited the rotation speed of the metal bar to fewer than 20,000 RPM. In order to rotate the rod being atomized up to 18,000 RPM, an electric motor turned a stationary spindle using a belt pulley system. The stationary spindle was connected to the metal rod using a collar-shaped holding device termed a collet. The other end of the metal rod was held in place by rollers attached to the container designed to catch the molten spray [9].

The circuit of the original REP used electrical brushes to make contact with the rotating metal rod so that a high current could pass through the rotating electrode. Using a power source, the potential difference between the gap of the rotating electrode and the tungsten stinger was increased until the air was ionized and turned into plasma. This process established an arc that provided the heat source to melt the rotating tip. Alternative heat sources were considered such as plasma torches, flames, lasers, and induction devices, but out of this set only plasma torches worked well enough to use in future designs. As the rotating electrode was consumed (i.e. atomized) it was continuously fed into the stationary tungsten stinger by moving a sled holding the stationary spindle and motor towards the container holding the tungsten stinger [9].

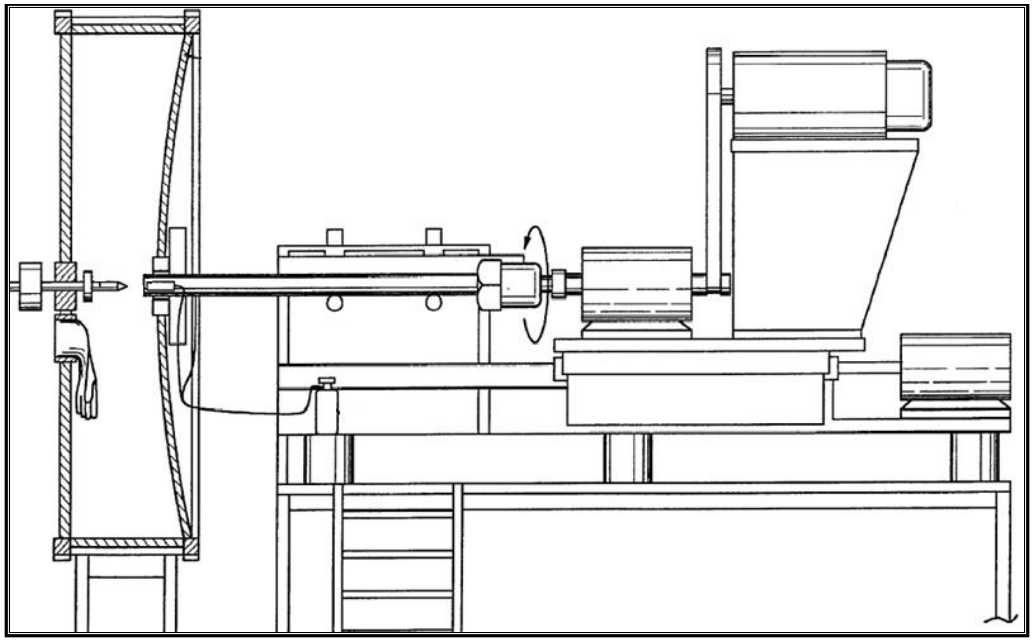

Figure 2-10: The rotating electrode process by Starmet Corporation [9].

The entire process was carried out in an inert environment to prevent oxidizing the powder. This was done by pressurizing the container with an inert gas such as argon. The whole machine could be placed in an inert environment if the electric motor was modified to operate in the inert gas [9].

2.3.3 Idaho National Laboratory REP Design

Idaho National Laboratory (INL) designed a somewhat similar machine based on Starmet's rotating electrode process and named it the laboratory scale fuel atomizer. The atomizer was built to produce U-7Mo powder that would be used to fabricate fuel as part of the Reduced Enrichment for Research and Test Reactors (RERTR) program. The U-7Mo was chosen because of the promising results demonstrated when dispersing it in a

silicon doped aluminum matrix. The atomizer went through various changes as it evolved from a trial and error process, with the final design being depicted in Fig. 2-11 [10].

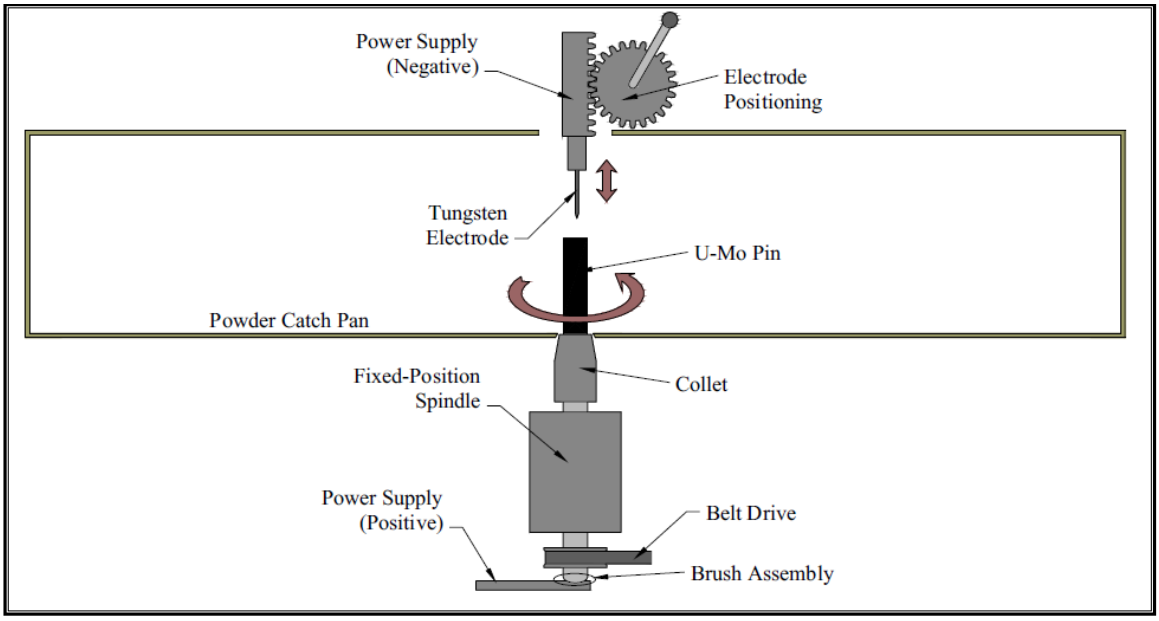

Figure 2-11: The INL fuel atomizer [10].

There are three key differences in the final design of the INL fuel atomizer that make it significantly different from the original and commercial REP system created by Starmet. First, it is vertically oriented to allow for easier operation in the specific glove box into which it was installed. Secondly, the tungsten stinger is fed into the vertically oriented rotating electrode (instead of feeding the rotating metal toward the stationary electrode) to reduce alloy waste and allow for greater stability while rotating at higher RPMs. Lastly, the INL fuel atomizer is designed to reach RPMs of over 40,000,

compared to 18,000 for commercial REP's, enabling the production of smaller powders [4].

The design uses a motor to rotate a stationary spindle using a belt pulley system similar to the original REP. A Dumore Corporation tool post grinder (model 8473) normally has a grinder wheel attached to the stationary spindle, but was retrofitted to spin a 0.635 cm (0.25 in) diameter collet that can hold a U-Mo pin. The modified tool post grinder was then mounted on a large post in such a way that the collet faced upwards, allowing for the vertical orientation. This post was attached to a large metal disk to alleviate vibration during operation. The modified system can be seen in Fig. 2-12 [4].

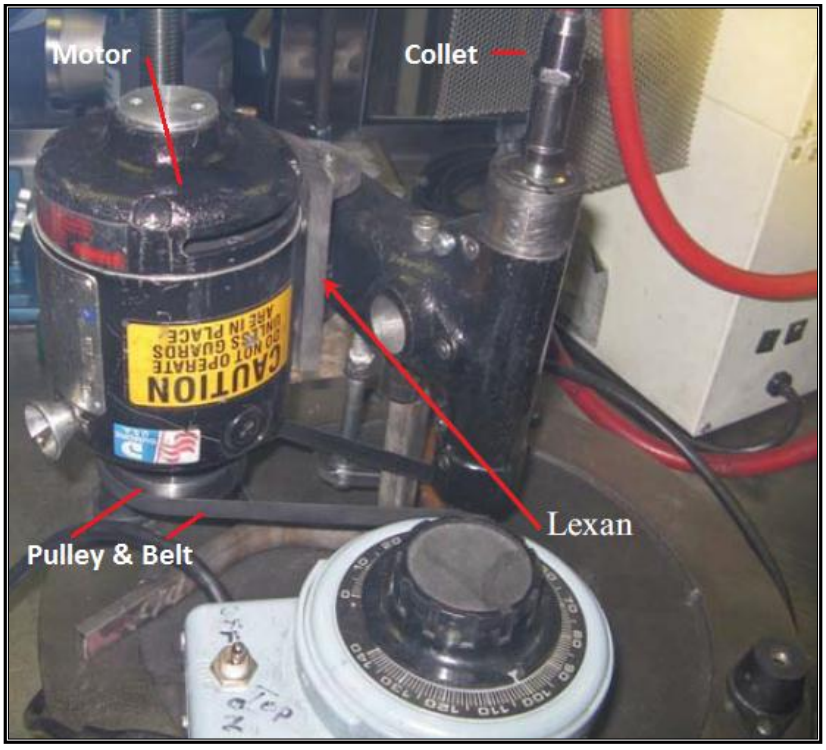

Figure 2-12: The INL fuel atomizer motor with modifications noted [4].

The stationary spindle has a rod extending from the opposite side of the collet which is attached to a copper stud that makes contact with two graphite brushes held in place by a copper brush holder. The brushes provide the electrical contact between the rotating pin and the power source, a TIG welder. Figure 2-13 displays this copper stud in contact with the graphite brushes [4].

Figure 2-13: The INL fuel atomizer brush system [4].

A collection chamber is placed over the collet and supported in place while the pin is allowed to spin freely. The chamber is a 35.56 cm (14 in) diameter stainless steel cylinder that is ~10 cm in height that is designed to catch any molten material propelled during atomization. The top lid is made of Lexan, a clear non-conductive high temperature polymer so that the operator can see into the collection chamber during operation. This ensures that the tungsten stinger is the proper distance from the rotating

electrode to maintain the arc during atomization. Figure 2-14 displays the collection chamber.

Figure 2-14: The INL fuel atomizer collection chamber without lid [4].

The tungsten stinger was a ~0.48 cm (3/16 in) diameter tungsten electrode that is normally used for TIG welding. Since the TIG welder can be grounded to the electrical brushes, it didn't need any modifications for this system. The tungsten electrode was to be mounted to a Dremel Work Station Model 220 rack and pinion system which allowed the operator to move the stinger up and down using a crank [4]. As the rotating electrode was consumed (i.e. atomized), the operator moved the tungsten electrode to maintain ~1.25 cm separation distance which could be seen through the Lexan cover. The welder used was a Miller Maxstar 350 welding system. The current was set to DC, and melting

of a 0.95 cm (3/8 in) diameter U-7Mo began around 75A. The operator used a foot amp troll to control the current [10].

2.3.4 Results & Correlations from Prior Systems

The particle size distribution depends on the properties of the liquid metal, centrifugal forces, and aerodynamics of the ejected liquid metal through the inert gas. The median particle size based on material properties and RPM is predicted by

$$d = \frac{0.000346k}{\omega}\sqrt{\frac{\gamma}{\rho D}} \tag{2-1}$$

where d is the median particle diameter (μm), ω is the rotating rate (rads/s), γ is the surface tension (dynes/cm), ρ is the density (g/cm^3), D is the diameter of the electrode (cm), and k is an empirical constant principally determined by the method of droplet formation which is in turn controlled by the melting rate [8]. Since any given alloy being atomized will have fixed material properties, Eq. 2-1 can be simplified down to

$$d = \frac{K}{\omega\sqrt{D}} \tag{2-2}$$

where K is a material constant (over a limited melting rate range) that has been determined for many alloy systems [11]. In order to characterize the REP size distribution for U-Zr alloys, K needs to be determined.

Powders and fabrication data from the original REP system described above demonstrated the accuracy of the above correlations. For example, 1018 steel and titanium alloys were atomized and the resulting size distributions are displayed in Fig. 2-15 [8]. The correlations shown in Eq. 2-1 and 2-2 predict a decrease in median particle size as rotation speed increases, which is clear from the size distribution shown in Fig. 2-15.

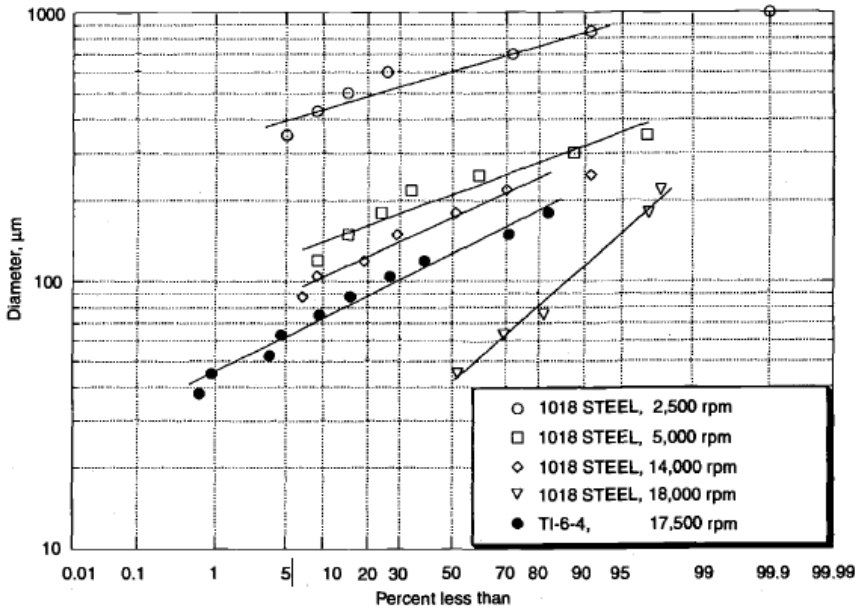

Figure 2-15: The effect of rotation speed on steel and titanium alloy particle size [8].

The U-7Mo particles produced by INL had a fairly tight size distribution, which quickly shifted towards a smaller median diameter when the RPM was increased. This distribution is shown in Fig. 2-16, with 120V providing the voltage to rotate at 35,000 RPM and 140V for 45,000 RPM (measured unloaded) [12]. The particles themselves were spherical in shape and displayed no signs of constituent segregation. The clumping

that did occur was because of either insufficient separation of molten droplets prior to solidification or the droplets collided in flight and coalesced prior to solidification [10]. Figure 2-17 displays the U-7Mo particles produced [10]. X-ray diffraction checked the particles to see if segregation had occurred. Figure 2-18 displays the results of the X-ray map [10], which shows a homogenous mixture indicating that no segregation occurred.

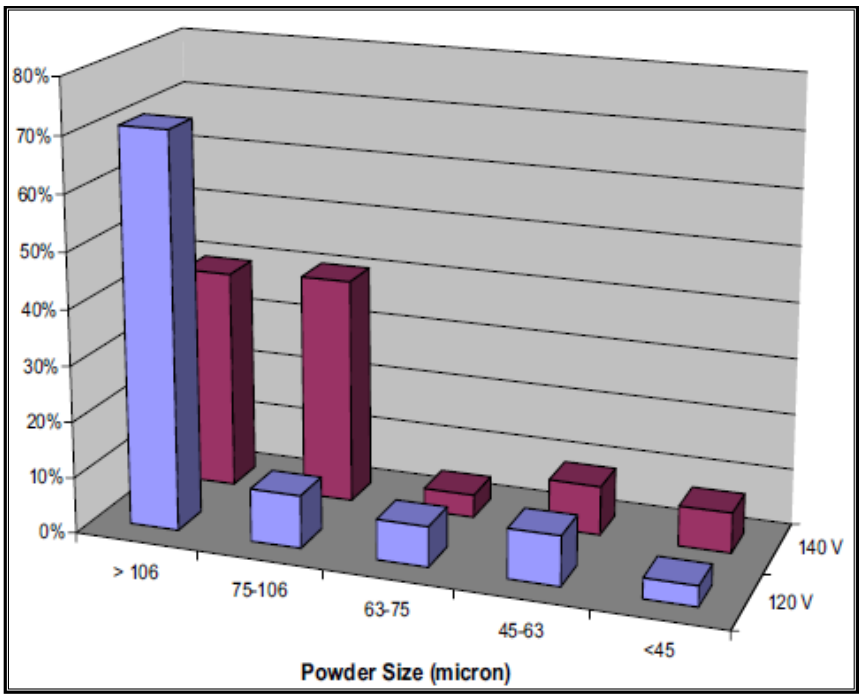

Figure 2-16: The effect of rotation speed on U-7Mo particle size [10].

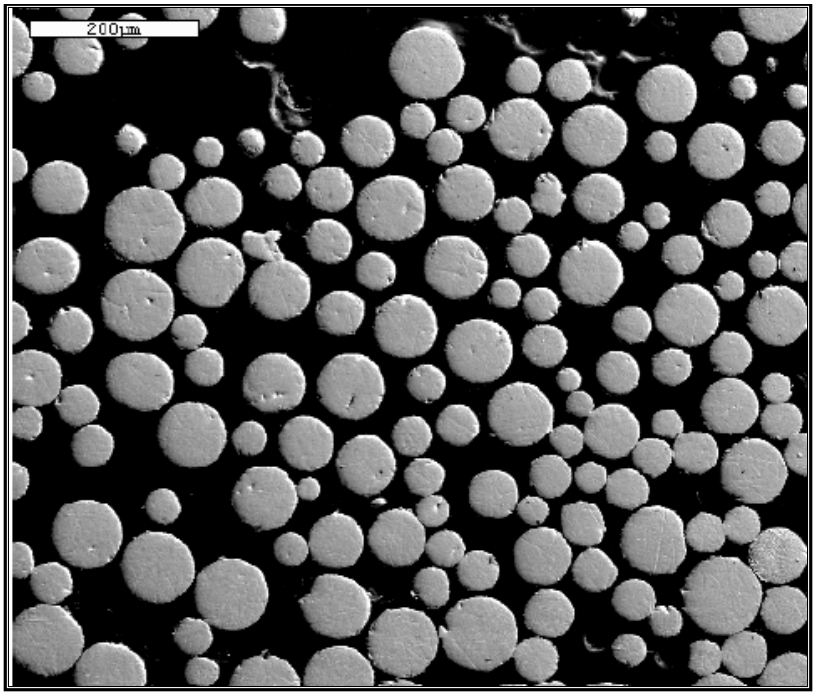

Figure 2-17: Polished U-7Mo particles produced using INL's fuel atomizer [10].

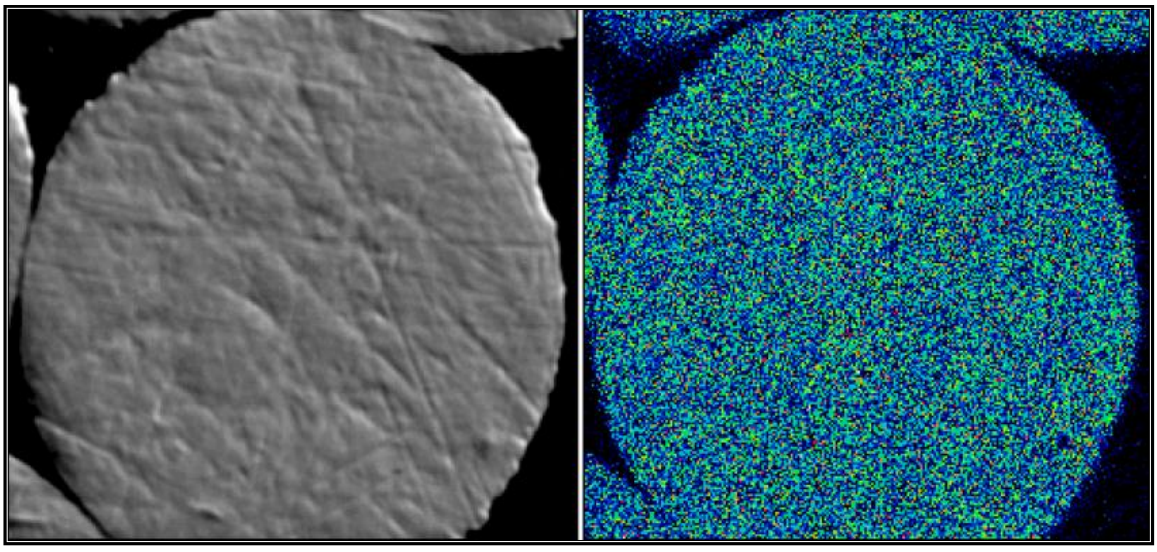

Figure 2-18: SEM photograph compared to X-ray map of a U-7Mo particle [10].

3. DESIGN AND ASSEMBLY OF THE TAMU RES

The design of the Rotating Electrode System established at Texas A&M University is presented in this chapter. This includes a summary of the assembly procedures, and installation of each major component. Each component is described sequentially in the order of assembly. Each section contains a general description of the component followed by item specific design discussions and a summary of fabrication, installation, and/or programming instructions.

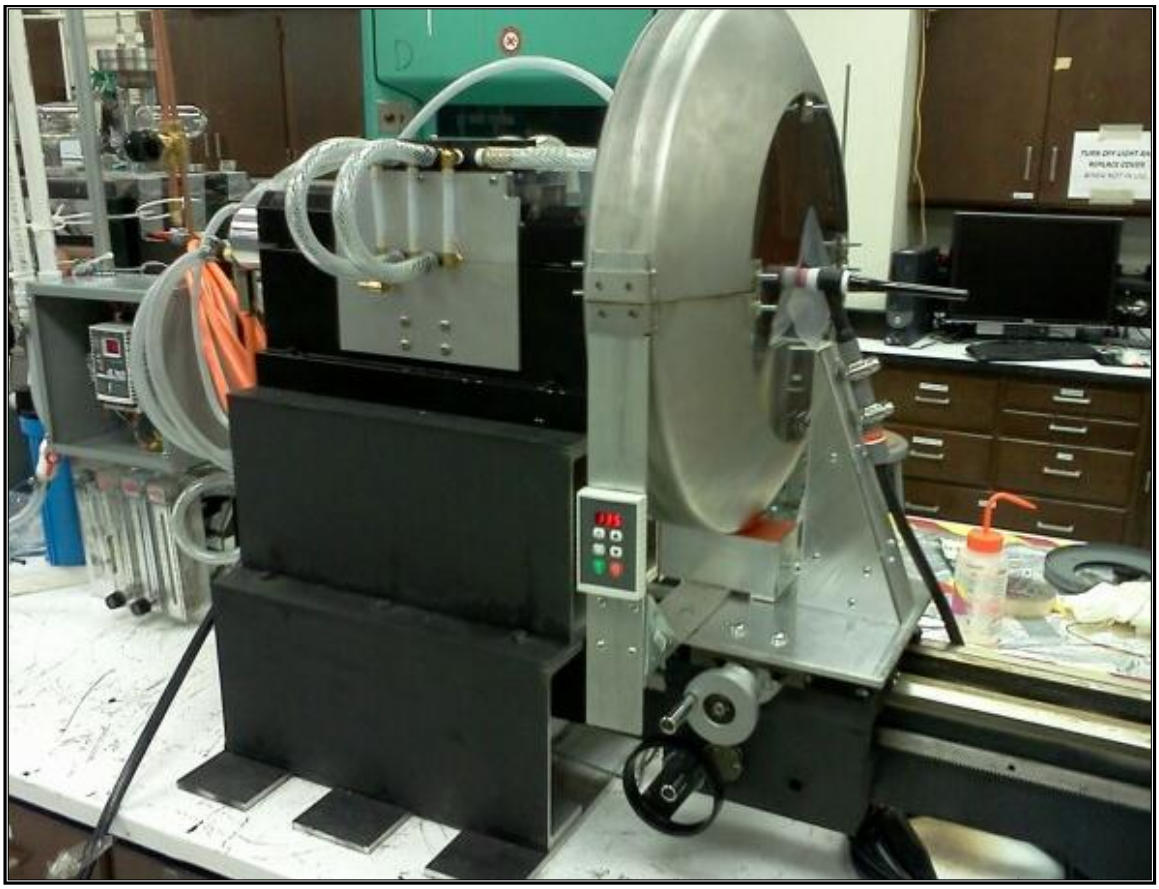

Figure 3-1: The Rotating Electrode System.

The completed TAMU RES, seen in Fig. 3-1, uses aspects from both the original Starmet REP design and the INL fuel atomizer. It is designed to atomize alloy rods with diameters up to 1cm (~0.5 in) with rotation speeds up to 40,000 RPM. This is accomplished by melting the tip of the rotating electrode using an electric arc. As the pin melts, centrifugal forces will overcome the surface tension of the molten metal and propel droplets radially and the liquid drops will solidify in flight into microspheres. These microspheres will then hit the walls of the catch pan which surrounds the rotating pin. The microspheres will be collected at the bottom of the catch pan.

A horizontal orientation was selected (similar to Starmet, but different from INL) so that the microspheres would fall to the bottom of the vertically oriented catch pan. The microspheres pass through a bottom hole in the catch pan into a removable drawer, allowing for easy removal from the system. In addition, the RES device is designed to be installed inside an inert atmosphere glovebox (not part of this document).

3.1 Electrical Brushes

The first components to be discussed are the electrical brushes that enable the flow of high current through the rotating rod. The brush choice, either directly or indirectly, affects the design of nearly every component. The use of electrical brushes is common for transferring a signal or current into a rotating shaft, known as a slip ring. The brushes are not actual brushes, such as a paintbrush, but solid contacts that are pressed against a lubricated slip ring while it is being rotated.

The brushes may be made from several materials, and the selection must be based on the optimal combination of current density and allowable surface speed between the brush and slip ring. The RES is intended to rotate at high RPM's so only graphite or electrophatic brushes were considered since the offer the highest surface speeds, which becomes important in the slip ring design. These brushes can function at surface speeds of up to 100m/s [13].

Mersen (Philadelphia, PA, U.S.A.) is an industrial manufacturer of electric brushes and holders. They recommended an electrographitic brush (part number LFC554) that is normally used in synchronous machines. It is capable of operating continuously at a speed of 90m/s while transferring 10A/cm^2 [13]. It was recommended this grade of brush be used in conjunction with a stainless steel slip ring due to the strength and rigidity of stainless steel. The rotation speed of the slip ring was used to set the slip ring diameter to ensure a surface speed of 90m/s is not exceeded (see Section 3.3). However, for a slower operation a different brush material may be a better choice. A tabulated list of various brush materials with operating parameters can be found in Appendix A.

The size and number of brushes was determined by the contact area required to transfer the desired current. The INL fuel atomizer required 75A before the tip of a 0.95 cm (3/8 in) U-7Mo pin began to melt [4]. The RES was designed so that a slightly larger pin can be atomized, so the brushes were designed conservatively to be able to transfer up to 200A during operation. Since the LFC554 has a rated current density of 10A/cm^2, the total maximum contact area required is 20cm^2. Mersen recommended that this area

be divided into 10 brushes to spread the heat being generated over the slip ring surface area and that each brush have the dimensions depicted in Fig. 3-2.

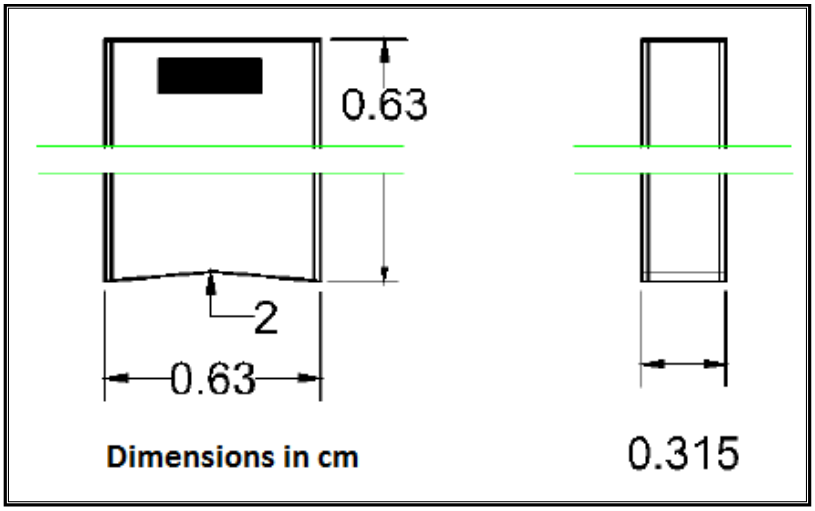

Figure 3-2: The dimensions of the electrographitic brushes manufactured by Mersen.

The brushes were recommended to be applied with contact pressure of ~2.1 N/cm^2 (~3 psi) in order to maintain constant contact with the slip ring, which will generate significant frictional losses. These frictional losses can be determined by the applied pressure of the brushes and the coefficient of friction between the brushes and the slip ring. The LFC554 brushes have a coefficient of friction of 0.12 on stainless steel, which means the frictional losses from the brushes can be determined to be 4.97 N (~1.1 lb_f) by

$$F = P \times A \times \mu = 2.07 \frac{N}{cm^2} \times 20 cm^2 \times 0.12 \quad (3\text{-}1)$$

where F is the force, A is the contact area of the brushes, and μ is the coefficient of friction [13]. The large friction force from the brushes is more significant than the frictional losses from the bearings of the non-motorized spindle. Other frictional losses in the system are negligible in comparison. The motorized spindle must be powerful enough to overcome the frictional losses at full RPM and is discussed in section 3.4. The cooling system must also cool the heat generated from the friction of the brushes on the slip ring, which is discussed in section 3.3.

The brushes are designed to fit into holders designed by Mersen. The holders are then mounted on a copper stud, discussed in section 3.2. The brushes themselves are considered consumables, so seven sets were ordered. A single brush is depicted in Fig. 3-3.

Figure 3-3: A single LFC554 electrographitic brush fabricated by Mersen.

3.2 Brush Holders

The DDO 168-37 brush holder is designed for the electrographitic brushes manufactured by Mersen with the dimensions depicted in Fig. 3-2. The brush holders are "V" shaped and designed to mount to a single 1 cm diameter stud whose center is 5.13 cm from the center of the slip ring, discussed in section 3.3. Each arm extends radially and is pulled into the slip ring with a 2.07 N/cm^2 (3 psi) constant pressure spring. This pressure keeps the brush riding on the slip ring during operation. Figure 3-4 depicts the brush holders, shown in blue, holding the brushes in place and riding on the slip ring.

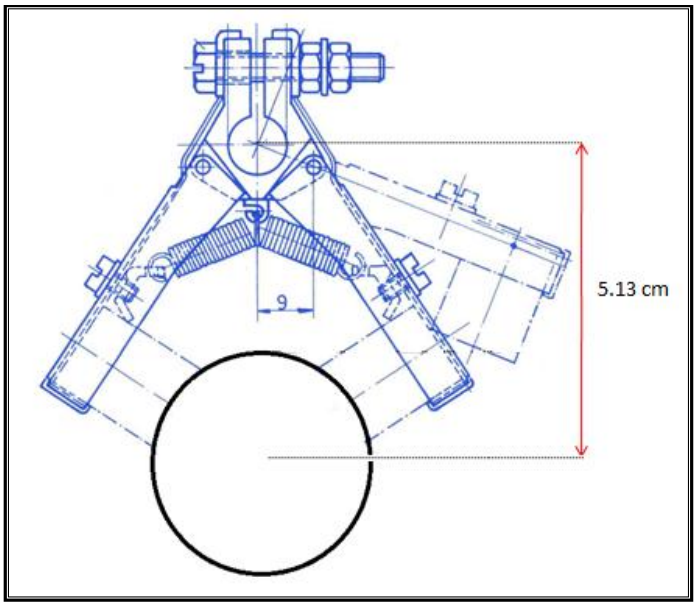

Figure 3-4: The DDO 168-37 brush holder riding on a slip ring [14].

The brush holders were mounted on a 1 cm diameter copper stud. The brushes were secured in the holders by screwing in the clamp shown in Fig. 3-5. The spacing of

the brush holders coincides with the lobes on the slip ring, which are discussed in section 3.3. Figure 3-6 depicts all five brush holders mounted on the copper stud.

Figure 3-5: How a brush is attached and secured to the holder.

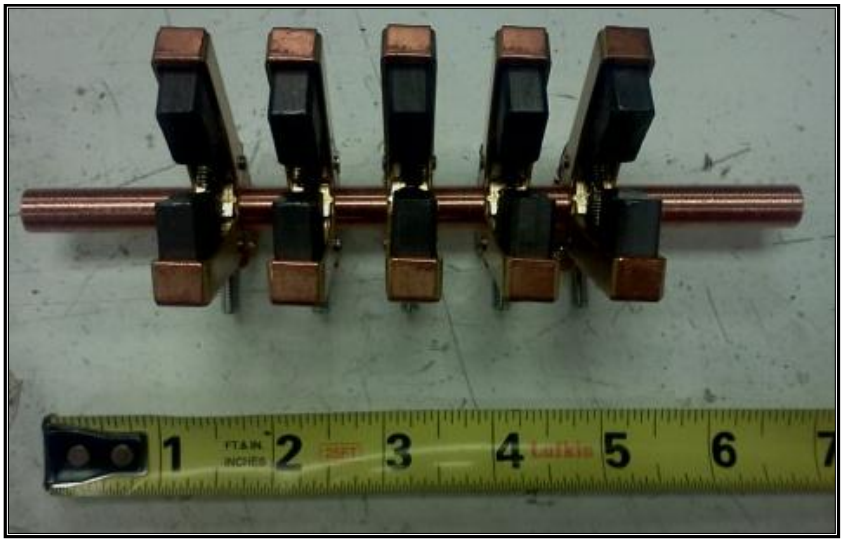

Figure 3-6: The five brush holders mounted to the 10mm copper stud.

3.3 Slip Ring & Cooling System

The slip ring is the rotating shaft that the electrical brushes ride on while transferring up to 200 A to the metal pin being atomized. The slip ring was designed in parallel to the slip ring cooling system since the length of the slip ring will be determined by the surface area needed for proper cooling. As section 3.1 discusses, a stainless steel slip ring was selected for two reasons. The first is to prevent run away oxidation as the slip ring is heated from friction with the brushes. The second is because stainless steel is strong, and structural integrity is assured if higher temperatures are reached. It is not expected that very high temperatures (above ~100 °C) will be reached due to friction, but steel remains a strong structural material up to ~500 °C.

The diameter of the slip ring is determined by the operating RPM's and the maximum permissible speed at which the brushes can operate. Since the LFC554 brushes are rated up to 90 m/s and the slip ring will be rotating at 40,000 RPM, the maximum diameter of the slip ring was determined to be 4.2971 cm (1.94 in) by rearranging the circumference of a circle multiplied by the RPM

$$D = \frac{90\frac{m}{s} \times 60s}{\pi \times RPM} \tag{3-2}$$

where D is the diameter.

The length of the slip ring is determined by the surface area is required for cooling. The amount of cooling depends on the heat being generated from friction losses and the voltage drop from the brushes to the slip ring. The LFC554 brushes on stainless

steel are expected to have a 2.3 V contact drop at full power due to the increase in electrical resistance between the contact of two different materials [13]. Using Ohm's Law, 460 W of heat is being generated through the contact, determined by

$$P = V \times I \tag{3-3}$$

where P is the power (W), V is the voltage (V), and I is the current (A). At full speed, 448 W of heat are being generated from friction losses, as determined by multiplying the force required to overcome the friction and the relative surface velocity of the contacts.

$$P = \frac{RPM}{\frac{60s}{minute}} \times \pi \times D \times 4.97N \tag{3-4}$$

where D is the diameter of the slip ring and 4.97 N is the friction force determined in section 3.1. This totals to 908 W of heat being generated over the slip ring surface area which could significantly heat up the ring if these calculations are accurate and all of the heat remains in the metal.

Because of this, it was determined that a forced convection cooling system for the slip ring surface was required for sustained operation. Forced convection during high speed can cool the slip ring if enough surface area is exposed to ambient air. The Nusselt number for a rotating cylinder in ambient air is

$$\overline{Nu} = \frac{h_c d}{k} = 0.11(0.5Re_w^2 + Gr_d \times \mathrm{Pr})^{0.35} \quad (3\text{-}5)$$

where Nu is the average Nusselt number (unitless), h is the coefficient of convection (W/m^2-K), d is the slip ring diameter (m), k is the thermal conductivity of air (W/m-K), Re_w is the peripheral speed Reynolds number (unitless), Gr_d is the Grashof number (unitless), and Pr is the Prandtl number(unitless) [15]. The peripheral speed Reynolds number can be determined by

$$Re_w = \frac{\pi \times d^3 \times w}{v} \quad (3\text{-}6)$$

where w is the peripheral speed (radians/s) and v is the kinematic viscosity of air (m^2/s) [15]. The Grashof number can be determined by

$$Gr_d = \frac{g \times \beta \times \theta \times d^3}{v^2} \quad (3\text{-}7)$$

where g is the acceleration due to gravity (9.81 m/s^2), β is the thermal expansion coefficient (1/K), θ is the temperature difference between the slip ring and ambient air (K), and v is the kinematic viscosity (m^2/s) [15]. The maximum difference in temperature was set to 100 K, so that the slip ring and brushes would operate near 200°C, well below the 600 °C auto-ignition temperature of graphite in air [16].

Therefore, a 400°C safety buffer is built in for the brushes since the slip ring can operate at much higher temperatures than the brushes.

Once the coefficient of convection was determined, the surface area and therefore the length of slip ring could be determined. Table 3-1 tabulates the aforementioned properties for air at -30°C, and calculated values. This lower temperature was used since since there will be a vortex tube ejecting cold air into the sealed slip ring area, and the air properties for heat transfer are worse at this lower temperature than at ambient air temperature.

Table 3-1: The calculated results for determining the slip ring length.

Variable	Value	Units
w	4188.79	rads/s
Pr	0.72741	
v	1.08E-05	m^2/s
k	2.17E-02	W/m-k
B	0.004113	K-1
d	5.08E-02	m
Gr	4.53E+06	
Re	3.14E+06	
Nu	3.05E+03	
h	1.30E+03	W/m^2-K
q	2.08E+04	W/m
l	4.37E+00	cm

The results show that roughly 5.08 cm (2 in) of slip ring surface area is required in order to cool the 908 W. However, there is uncertainty about the accuracy of this correlation since it was determined at a smaller angular velocity. Therefore, fins were

added to the slip ring design and the impinging jets of cold air were directed onto those fins. The fins were produced by spacing the 5.08 cm length of slip ring into five ~1 cm segments that the brushes ride on with roughly equal gaps where the slip ring diameter is reduced to a 1.95 cm (0.75 in) diameter. Therefor each fin will serve as a distinct track where two brushes will slide and the total slip ring length that is exposed to cold air is 10 cm (total length is accounted for by the two sections held by the collets). The jets of cold air were directed to the slip ring by interchangeable spray nozzles so that any optimization of the cooling system would be easy if it were warranted in the future.

The slip ring was machined out of 303 stainless steel since it is relatively easy to machine compared to other stainless steels and has favorable corrosive properties at higher temperatures [17]. A 5.4 cm (17/8 in) diameter 303 stainless steel cylinder was machined to a diameter of 5 cm (1.97 in) and helical grooves were added to ensure the brushes have a flat contact surface and to remove any hot gas trapped between the brushes and the slip ring [18]. This was done by scoring the cylinder 0.076 cm (0.03 in) in while setting the lathe machine to automatically feed 4 in per revolution. The cylinder was then polished using 400 grit sandpaper and the diameter was reduced to 1.9 cm (0.75 in) diameter every 1 cm using a plunge bit to form the fins. Finally, the ends were reduced to 1.25 cm for 3.18 cm so that the slip ring could be inserted into the collets. The complete procedure can be found in Appendix B. As fabricated, the slip ring weighs 0.87 kg (1.91 lb), and measures 13.97 cm (5.5 in) in length. Figure 3-7 shows the fabricated slip ring mounted between two collets.

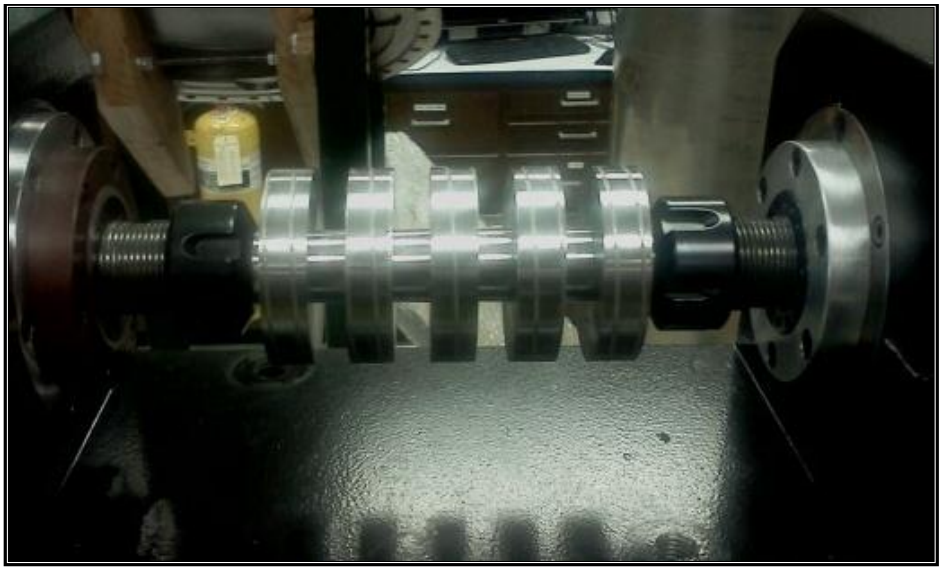

Figure 3-7: Photograph of the slip ring mounted between the two collets.

For the slip ring cooling system, the spray nozzles were placed ~0.5 cm from the slip ring surface. The brush holders are held in place by the copper stud above the slip ring, so the coolant spray nozzles must enter from the side of the slip ring. Two spray nozzles per track, with one per brush, were chosen to maximize the cooling rates if the jets are ever required. Figure 3-8 illustrates this cooling system.

The gas nozzles selected have a flat spray pattern. The first version of the spray nozzles will have a 30 degree horizontal spread, 0.25 cm (0.1 in) orifice diameter, and a flow rate of 2.27 E-3 m^3 (0.6 gallons) per minute at 551.6 kPa (80 psi) which is the pressure of the laboratory central air source. There are similar gas nozzles with higher flow rates so that system optimization could be easily accomplished if needed. Figure 3-9 depicts these spray nozzles.

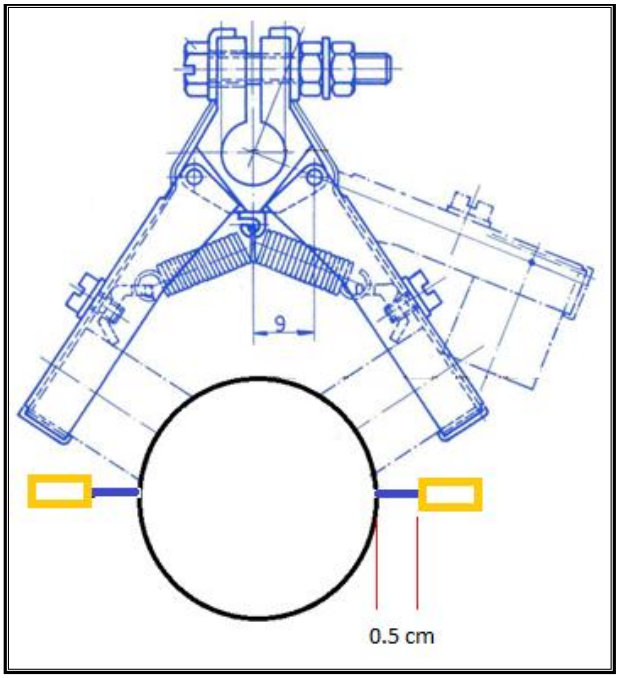

Figure 3-8: The location of the spray nozzles relative the slip ring [14].

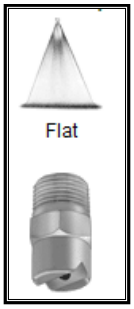

Figure 3-9: The spray nozzles selected to cool the slip ring [19].

The spray nozzles were mounted on aluminum plates that bolt to the spindle holder. Each plate then bolts to an insulated 1.25 cm thick high temperature polymer center piece. The center piece has one hole that a 0.61 cm in diameter bolt can connect the ground of the welder to the copper post clamp. The copper post clamp is a simple

aluminum flat bar with clamps on each end, shown in Fig. 3-10. The spray nozzles were spaced so that each one impinged on a lobe of the mounted slip ring shown in Fig. 3-11. The entire slip ring system bolts together using the three main pieces shown in Fig. 3-12.

Figure 3-10: The copper post clamp.

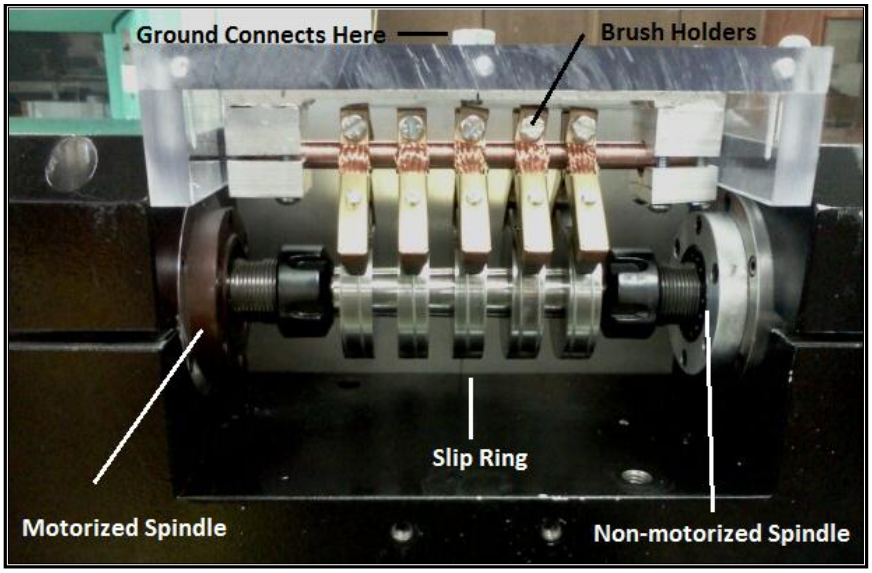

Figure 3-11: The slip ring mounted with one of the cooling system plates removed.

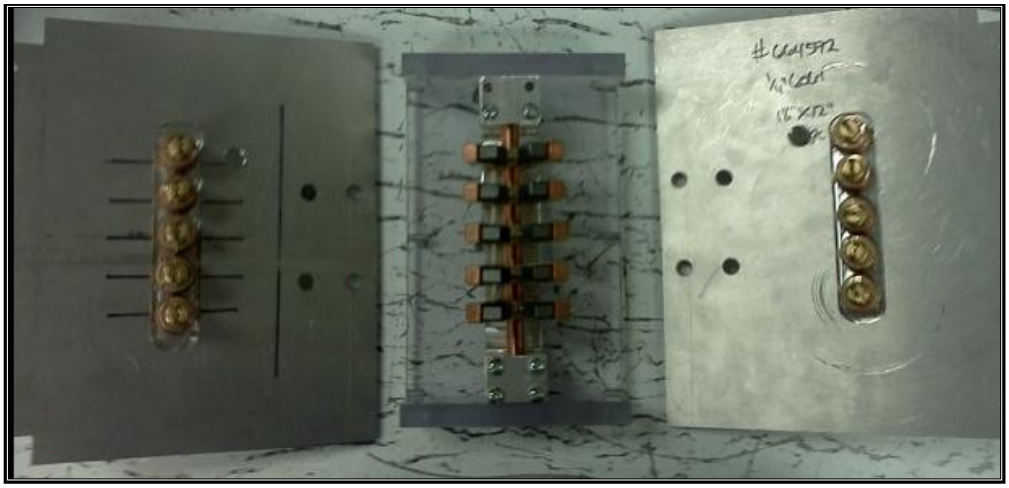

Figure 3-12: The slip ring system.

3.4 Spindles and Spindle Holder

The RES has two spindles mounted in a custom holder designed by Dynomax Incorporated. Two spindles were used so that the slip ring (Section 3.3) could be mounted between the two, alleviating vibrational harmonics resulting from imbalances within the slip ring. One of the spindles is motorized, while the other is not. The motorized spindle was fitted with a single 1.25 cm (0.5 in) collet, while the non-motorized spindle has two 1.25 cm collets – one on each end of a solid shaft. Each collet can be hand tightened when using a wrench to hold the shaft, shown in Fig. 3-7.

The motorized spindle was designed to operate up to 40,000 RPM. These speeds were required to produce 100 μm diameter U-7Mo powder at INL and should produce similarly sized U-10Zr powder [10]. Only the power requirement of the motorized spindle needed to be determined. This power is used to rotate the slip ring while it is in

constant contact with the electric brushes as well as the non-motorized spindle, which holds the metal pin being atomized.

The power of the motorized spindle was determined to overcome the frictional losses between the slip ring and brushes, but later optimizations may need to consider the frictional losses between bearings and the solid shaft of the non-motorized spindle. As section 3.1 determined, the frictional losses from the contact of the electrical brushes with the slip ring are 4.97 N while at 40,000 RPM and the frictional losses from the bearings are assumed negligible when compared with the brushes. When there is 4.97 N of friction force, 0.127 N-m of torque are needed to rotate the 5 cm diameter slip ring, which can be determined by

$$\tau = r \times F \tag{3-8}$$

where r is the radius of the slip ring (m) and F is the friction force (N) .

Dynomax Incorporated was the spindle manufacturer selected to fabricate the custom spindle. Per recommendation, a model 1860 motorized spindle coupled with a model 2000 non-motorized spindle in a custom holder were implemented into the design. The model 1860 motorized spindle is a three phase integral induction AC motor designed to operate at 460 V with a power curve depicted in Fig. 3-13. The model 2000 non-motorized spindle is similar in size and can rotate at the same speed. Its bearings are electrically insulated to prevent shorts from ceasing the bearings through fusion of point contacts (i.e. bearings to the bearing track).

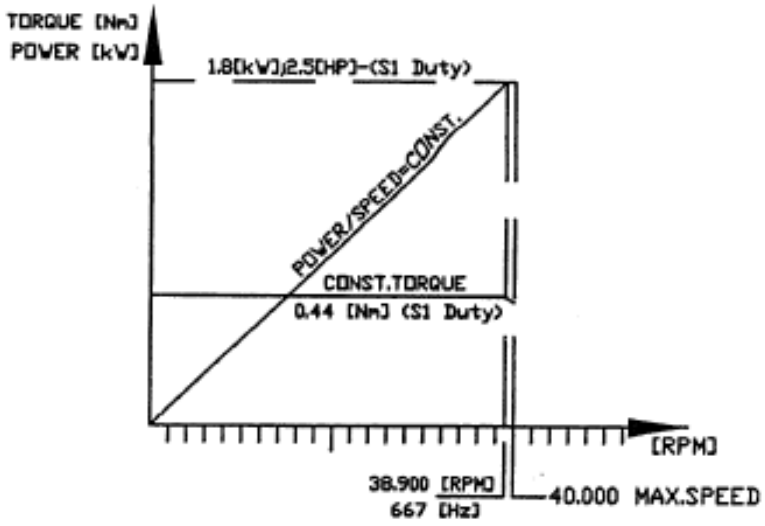

Figure 3-13: The power curve of the model 1860 motorized spindle.

As Fig. 3-13 depicts, the 2.5 hp model 1860 spindle is capable of rotating up to 40,000 RPM with 0.44 N-m of torque, which is estimated to be approximately four times more torque than needed. It was designed to be operated using a variable frequency drive (VFD), discussed in Section 3.5. It is both air and water cooled and mounted in a custom holder that aligns it with the Model 2000, shown in Fig. 3-14.

The holder design was based on the size of the spindles and the length of the slip ring. It was designed to accommodate a 10 cm (4 in) slip ring, discussed in Section 3.3. This holder has tapped holes so that the aluminum plates that hold the slip ring cooling system and center piece can be attached. The holder also has eye-hooks for transporting the very heavy holder in a glove box using a crane.

Figure 3-14: The two spindle holder.

An alternative design was considered that is similar to the INL's fuel atomizer that used a motorized double collet spindle. The spindle would require two pins extending in opposite directions; one would be the slip ring and the other would undergo atomization. A solid shaft would connect the two collets so current could be transferred from the slip ring to the U-Zr pin. However, after consulting Dynomax this concept was discarded since running 200 A through the solid shaft would interfere with an electromagnetic motor and belt-driven spindles are limited to ~30,000 RPM [20].

3.5 The Variable Frequency Drive

The Variable Frequency Drive (VFD) provides power to and controls the RPM of the motorized spindle. It controls both by adjusting the frequency and voltage supplied to the motorized spindle. The VFD must be matched with the operating

parameters of the motorized spindle, discussed in Section 3.4. Only the operating voltage, current, and frequency of the motorized spindle were needed when selecting a VFD. The frequency needed was determined using

$$RPM = \frac{f}{\#\ of\ poles} \tag{3-9}$$

where *f* is the frequency (Hz) [20]. At 40,000 RPM, a two pole spindle will operate at 667 Hz. Thus, the 2.5 hp Dynomax model 1861 motorized spindle operates using a three phase 460V input at 667Hz.

Dynomax recommended that the SF430V be used for this application (not to be confused with the SF430) manufactured by AC Tech Lenze (Uxbridge, MA, U.S.A.). This VFD operates on a 480Y input (i.e. three phase at 480V) and can power a 3 hp motor up to 999.9 Hz. A certified electrician mounted the VFD in the electrical enclosure box, shown in Fig. 3-15, that contains the in-line 10A breaker for surge protection. The 480Y input had four wires (L1, L2, L3, and ground) that need to be connected to the VFD using the diagram found in Fig.3-16.

Figure 3-15: The SF430V mounted in an electrical enclosure box.

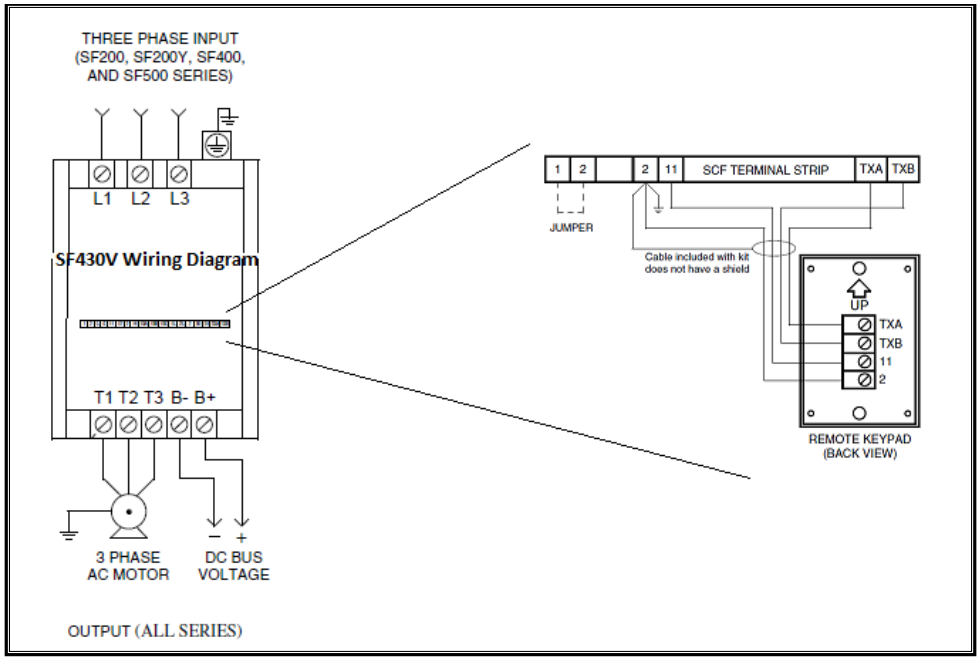

Figure 3-16: The wiring diagram for the VFD [21].

The motorized spindle used a proprietary cable that had one end screw directly into the spindle and the other end that needed to be wired directly into the output terminals of the VFD. The wiring diagram used to connect the spindle to the VFD is depicted in Fig. 3-17. The U, V, and W wires were attached to the T1, T2, and T3 output terminals respectively. The ground from the motor was attached to the input ground of the VFD power supply. The spindle thermoresistors must never be connected to the DC bus voltage outputs of the VFD or the spindle motor will immediately short out, permanently destroying its windings. During installation, a meter was used to identify each wire of the proprietary cable by measuring the resistance of each wire between the two ends as they were not identified on the VFD side.

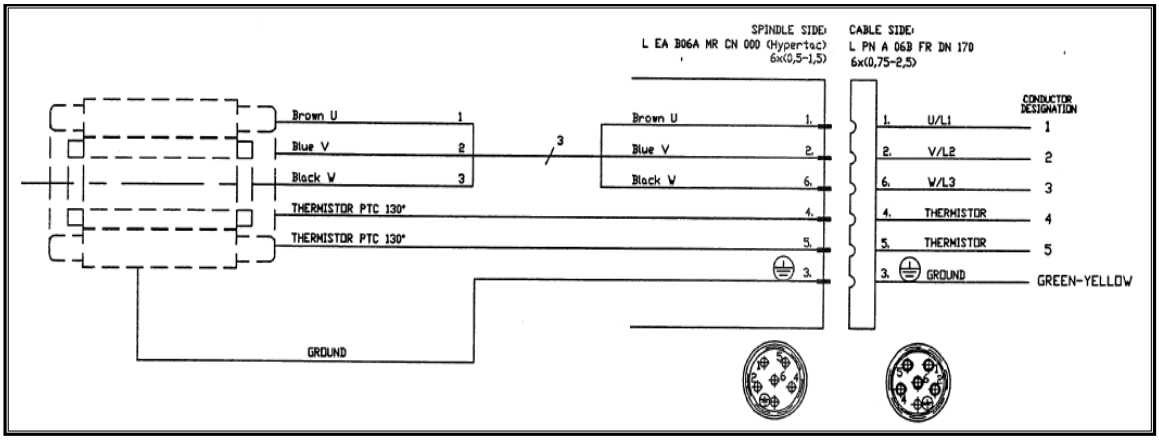

Figure 3-17: The wiring diagram to connect the spindle cable to the VFD.

A remote keypad was mounted on the catch pan column so that the operator does not have to leave sight of the tungsten stinger while changing RPM. Figure 3-16 was used to connect the keypad to the VFD. This keypad allows the operator to control

various parameters of the VFD such as starting the spindle, RPM, and stopping the spindle. The keypad turns on with the VFD once the breaker shown in Fig. 3-15 is closed. The VFD will automatically power up in the “off” position until the “run” button is pressed on the remote keypad. Figure 3-18 depicts the remote keypad.

Figure 3-18: The VFD remote keypad.

The VFD may be programmed using the remote keypad. Simply press the “mode” button on the keypad, followed by the password (1.2), and access to all the parameters is granted. Simply use the up and down arrows to guide to the desired

parameter and press “mode” to adjust the setting [21]. A complete list of parameters used can be found in Appendix C.

3.6 The Catch Pan and Drawer

The catch pan was designed to catch all metal powders produced by the RES as well as contain the argon cover gas. The molten material propelled from the alloy pin by centrifugal forces is expected to solidify before it hits the wall of the catch pan. Therefore, the vertical orientation of the catch pan enables the powder to collect at the bottom, where it will fall through a hole into a drawer. The drawer can easily be removed so that the powder can be transferred out of the glove box with ease. The catch pan was manufactured at Bryan Custom Fabricators using the procedure found in Appendix B.

The catch pan itself is a 50.8 cm (20 in) diameter psuedo cylinder that is 15.24 cm (6 in) in depth and can be seperated into two pieces, shown in Fig. 3-19. Both pieces were mounted on 5.08 cm x 0.64 cm x 35.56 cm (2 in x 0.25 in x 14 in) support columns that attach to a cross beam using “L” brackets, which is attached to the carriage, shown in Fig. 3-20. All the pieces of the catch pan were bolted rather than welded so that they can be diassembled and transferred through the 35.56 cm (14 in) air lock.

Figure 3-19: The catch pan without inserts installed.

Figure 3-20: The catch pan column supports attached to the carriage cross beam.

The catch pan was designed with insert brackets so that custom inserts could be fabricated and swapped as needed. Inserts were connected to the front and rear face of the catch pan to prevent debris from leaving the catch pan and to allow the operator to see into the catch pan during operation. The front insert is made from alumunim sheet metal and has a 10 cm diameter hole in the center of it to allow the heat shield of the non-motorized spindle to enter. The tolerances are close to minimize argon leakage, shown in Fig. 3-21. An indentation on the top half of this insert accomodates the non-motorized spindle coolant tube so that the catch pan can can be moved as close as possible to the spindle holder, shown in Fig. 3-22.

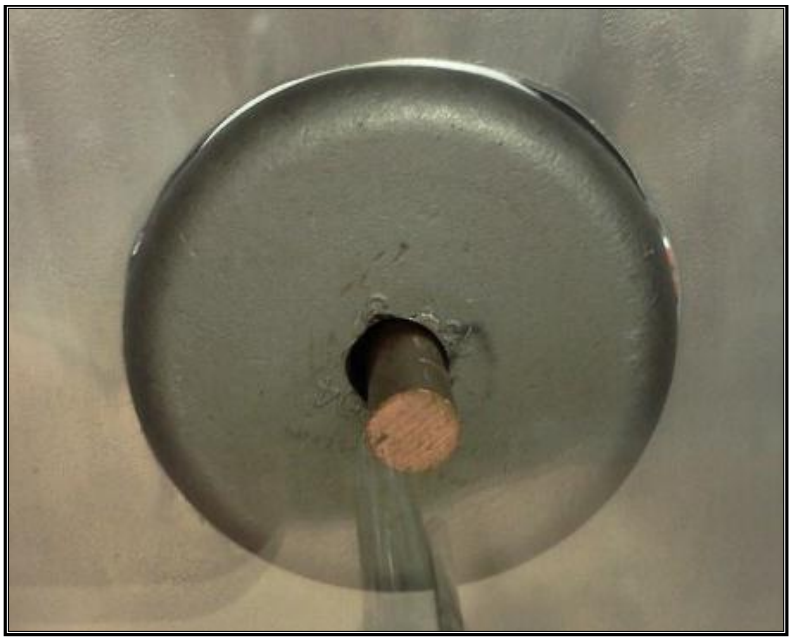

Figure 3-21: The front insert showing the small clearance avialable to the heat shield.

Figure 3-22: The front face insert indentation.

The rear insert is made from 0.95 cm thick high temperature, impact resistant polymer that has a 2.5 cm diameter hole for the tungsten electrode to enter. This insert is clear so the operator can see the location of the tungsten electrode relative to the rotating pin being atomized. This allows the operator to ensure that the two electrodes are the correct distance from each other to sustain the arc. Figure 3-23 depicts the rear face insert.

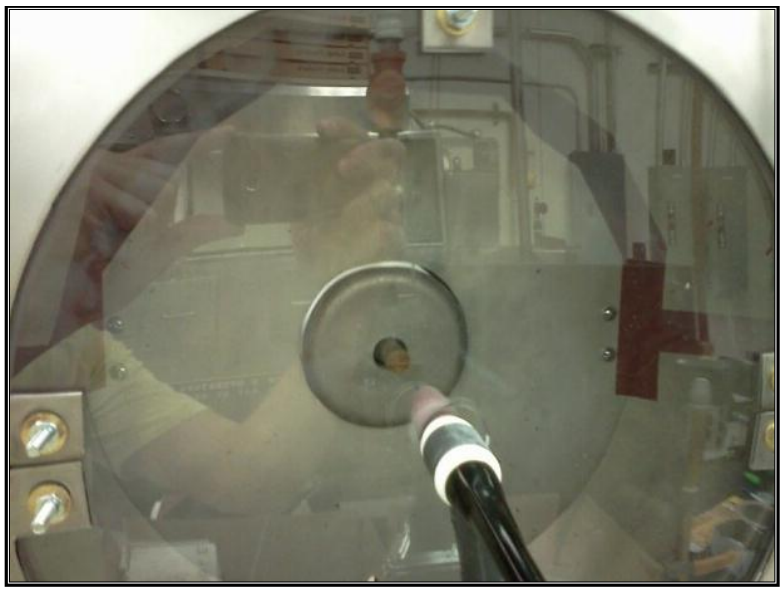

Figure 3-23: The clear rear face insert allows the operator to see into the catch pan.

The internal joints of the catch pan are sealed using a high temperature, silicon based anti-friction tape that sticks to the walls. This tape is applied through the 10 cm diameter hole on the front face insert. Figure 3-24 shows a photograph of the inside of the catch pan with the tape installed.

Figure 3-24: The silicon anti-friction tape over the joints inside of the catch pan.

An argon cover gas was injected into the catch pan assembly to alleviate oxidation of the powder during testing in an air enviornment; this feature will not be necessary once the unit is moved into an inert atmosphere glovebox. The argon was injected through wide angle defelected spray nozzles (120 degrees) attached to the top of the catch pan, shown in Fig. 3-25. Argon can also be injected through the sheath surrounding the tungsten electrode which is the common method to alleviate oxidation during operation for TIG welders.

Figure 3-25: The argon spray nozzles mounted to the top of the catch pan.

A drawer was designed and installed at the bottom of the catch pan and was fabricated to collect the microspheres that fell through the hole at the bottom of the catch

pan during operation. Latex was cut and glued to both the drawer and catch pan using RTV sealant to form a seal. There is a filter on the exhuast outlet of the collection drawer to minimize argon leakage through the catch pan. Figure 3-26 shows a picture of the drawer.

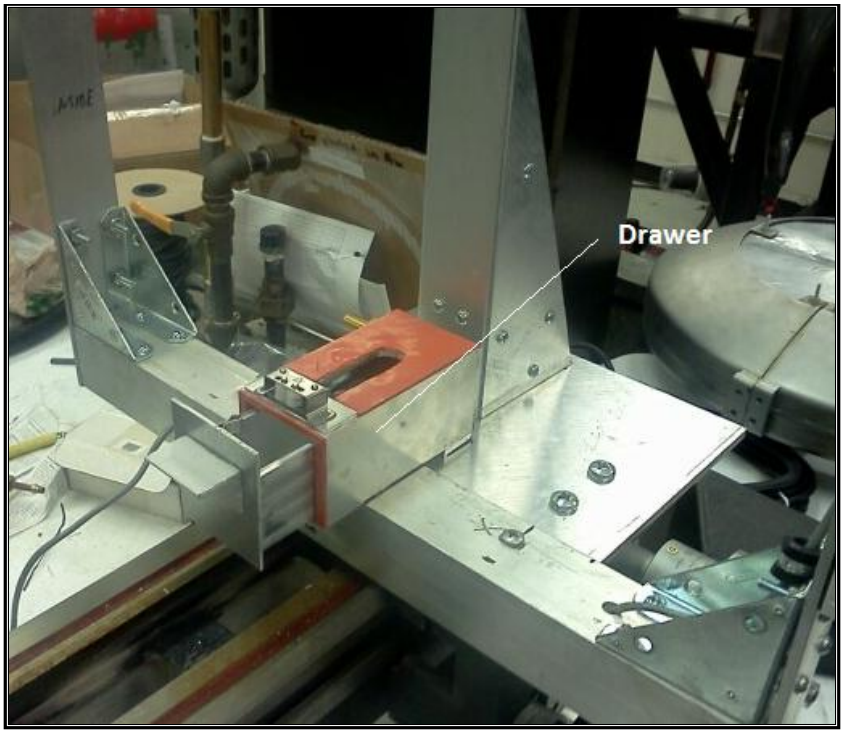

Figure 3-26: The drawer with the catch pan removed.

3.7 The Lathe Bed

The basic mechanical operation of this RES metal atomizer is based on a typical metal lathe operation similar to turning down a metallic cylindrical pin. As such, the atomizer was created to reside on a customized lathe bed; the commercial lathe bed component selected for this system is normally used on a G0516 combo lathe offered by

Grizzly Industrial Incorporated (Bellingham, WA, U.S.A.). The lathe bed was retrofitted so that an adapter plate could bolt flat against the "bed ways" which are the flat areas on top of the bed that the carriage glides along, shown in Fig. 3-27. This adapter plate is responsible for attaching the lathe bed to the spindle holder structure support. This assures the correct alignment of the spindles with the catch pan as the catch pan moves along the bed ways via the carriage.

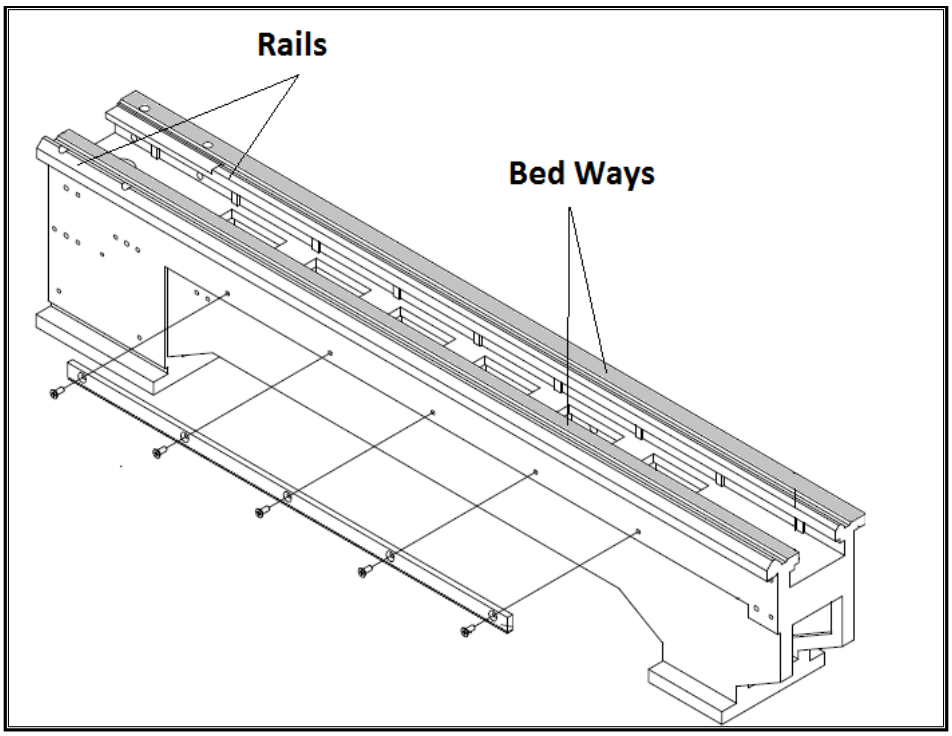

Figure 3-27**:** The G0516 lathe bed by Grizzly Industrial Incorporated.

The lathe bed has to fit through the 35.56 cm (14 in) diameter airlock of the future glove box installation and provide enough travel for the carriage to allow for easy access to the collet of the spindle. Therefore, this particular component must pass

through with a fully open air lock since the length is much larger than a typical air lock can accommodate. The length of the bed was determined by how much of the bed the spindles will occupy and the size of the catch pan. The distance between the spindles front face to the catch pan cranked as far back as possible was set to allow easy access to the collet, roughly 40.64 cm (16 in). This will ensure any pins being atomized can be easily inserted or removed from the collet. However, the selection of lathe beds is limited to discrete sizes so a slightly shorter lathe bed was used and support structures were built for the section of spindle holder that extended past the edge of the lathe bed. Figure 3-28 illustrates the idea used in determining the length of the lathe bed. With a 43.18 cm (17 in) spindle holder, the lathe bed should be 114.3 cm (45 in) in length.

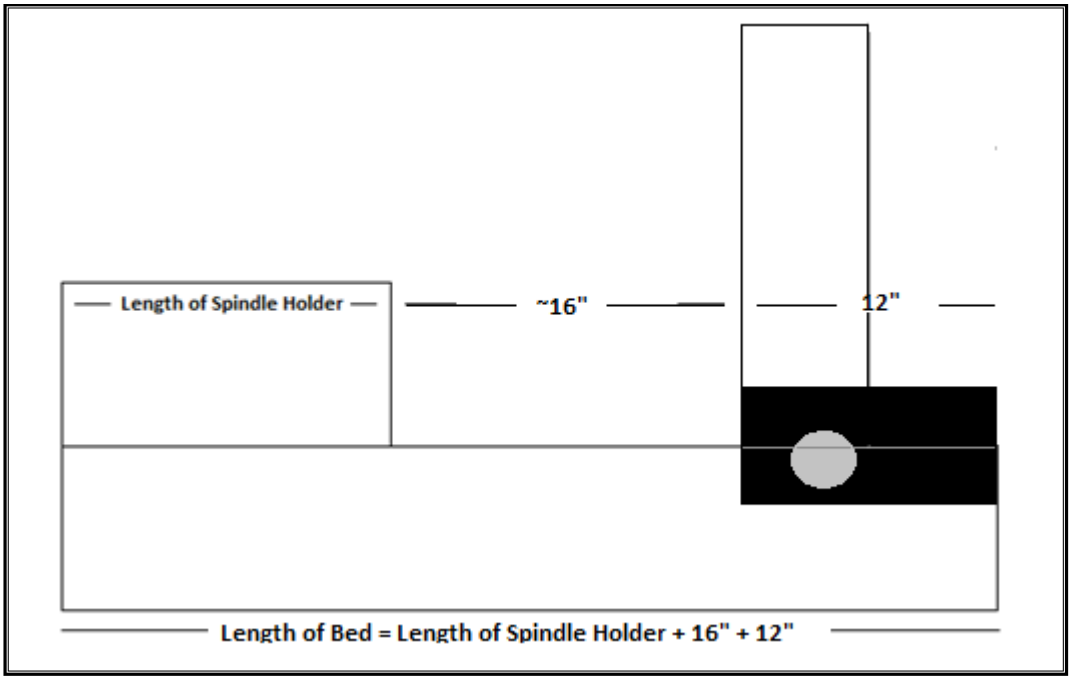

Figure 3-28: The determination of the length of lathe bed.

The stock lathe bed had typical rails on the bed ways that guide the carriage, shown in Fig. 3-27. These rails rise above the bed ways and inhibited the adapter plate from bolting flat and evenly to the bed ways, requiring removal of the rails.

The rails, as well as the bed ways, are flame hardened cast iron and are difficult to machine, and hence difficult to remove. In addition, finding a milling machine capable of handling such a large and heavy object is difficult proved to be costly. The simpler and cheaper solution used for removing the rails was to use a plasma torch and cut them off. Careful control of the torch angle was required and about a half inch of material was removed from each rail. Figure 3-29 depicts the approximate angle used to cut the rails off while Fig. 3-30 depicts the actual lathe bed after the cut.

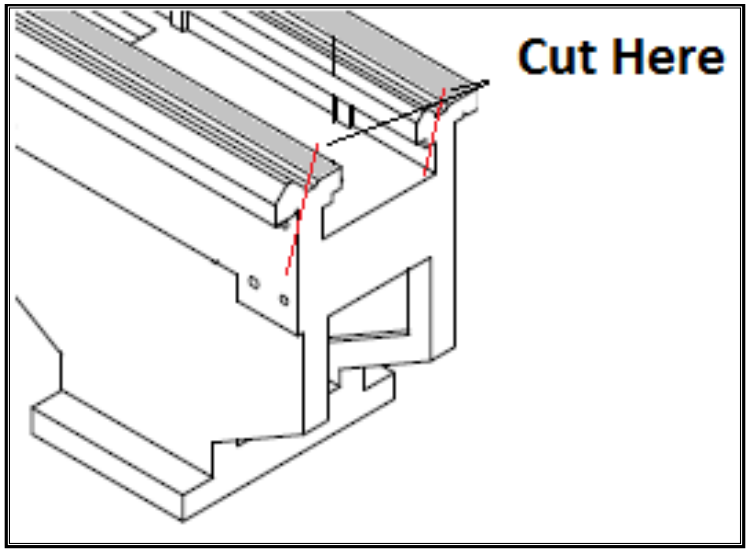

Figure 3-29: The approximate angle to cut the rails off of the bed ways.

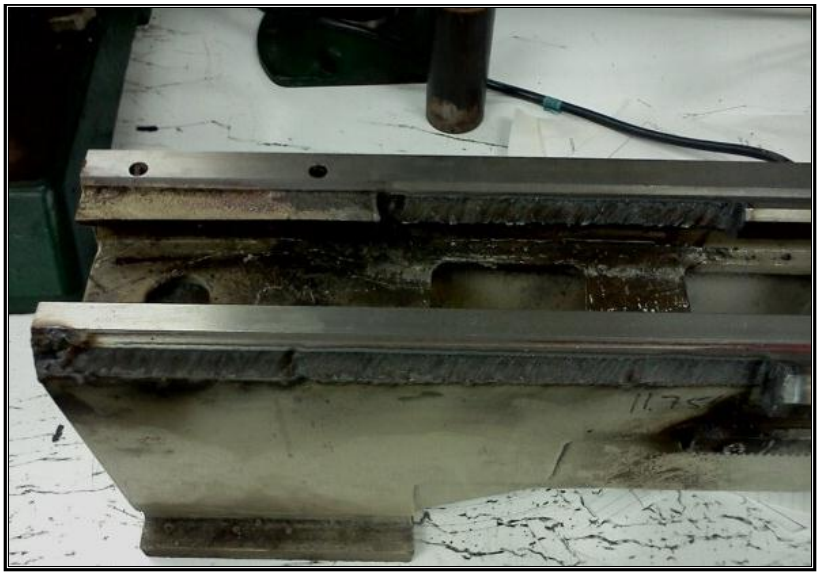

Figure 3-30: The lathe bed after a section of the rails was removed using a plasma torch.

3.8 Carriage & Catch Pan Support Columns

The carriage is the sliding assembly the catch pan is mounted on, as shown in Fig. 3-31. It glides along the bed ways and is guided by the rails of the lathe bed. The carriage used was matched to the lathe bed since it was a part of the original combo lathe. The operator moves the carriage by cranking a rack and pinion gear set. The complete list of parts required to assemble the carriage from Grizzly Industrial can be found in Appendix A.

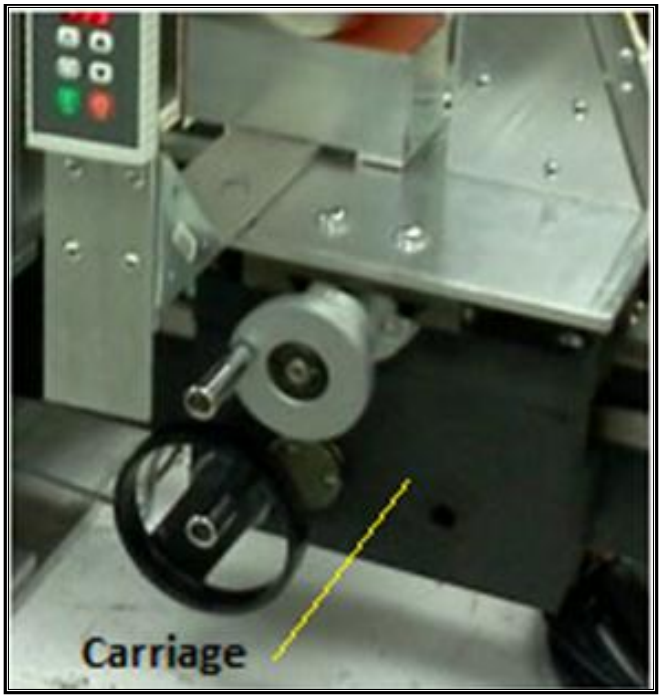

Figure 3-31: The carriage of the RES.

The lathe bed was altered since it did not come with pre-drilled holes for the rack to be bolted to. The holes were custom located by sliding the assembled carriage on the bed ways to the mid-point of where the rack should be, which will coincide with the section of the bed ways that still have the rails left from Section 3.7. The rack was placed on the correct side of the lathe bed so that it was in contact with the carriage gear and the edges were taped in place using duct tape. The carriage was carefully cranked using the hand crank along the lathe bed to ensure the carriage gear is in contact with the rack throughout the entire length of travel. Holes were marked on the lathe bed using a marker in each of the predrilled holes in the rack, drilled, and tapped. The rack was then, bolted to the lathe bed.

3.9 Power Supply & Torch Holder

The power supply to establish an arc between the rotating electrode and the tungsten stinger came from a TIG welder. The TIG welder was set to DC- mode with a specified current once incorporated into the RES. The current was kept constant throughout the process and the welder automatically adjusted the voltage to sustain the arc.

The only variable that needed to be determined when selecting the TIG welder was the duty cycle at the maximum operational current. INL's fuel atomizer required 75A to melt a 0.95 cm (3/8 in) U-7Mo pin, and so the minimum requirement set for the RES welder was a 100% duty cycle while running at 75A [10]. Since the RES was designed to atomize slightly larger pins, 200A was selected as the maximum operating current.

The Lincoln TIG-225 was chosen because it had a duty cycle of 100% while running at 90A DC and 40% while running at 200A [22]. This means the welder could provide 200A continuously for 4 minutes every 10 minutes, which at the time was expected to be far more time than needed (actual operation times were determined in Section XX to be less than 30s). Figure 3-32 depicts the welder chosen for the RES.

Figure 3-32: The Lincon TIG 225 welder used on the RES.

The welder came preassembled and only the torch head holder needed to be fabricated. The tungsten stinger needed to be 32.39 cm (12.75 in) from the carriage base to be centered in the catch pan, so a triangular holder was constructed out of aluminum that the torch head could be attached to via hose clamps, shown in Fig. 3-33. A triangular shape was chosen because the tungsten stinger is aproximately 120 degrees from the handle. Figure 3-34 illustrates this idea.

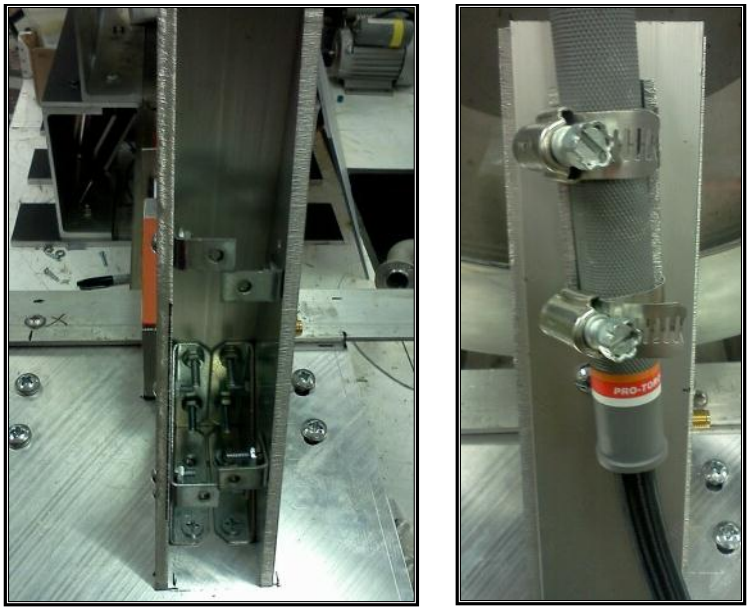

Figure 3-33: (left) The torch head holder without the top piece and (right) the complete torch head holder.

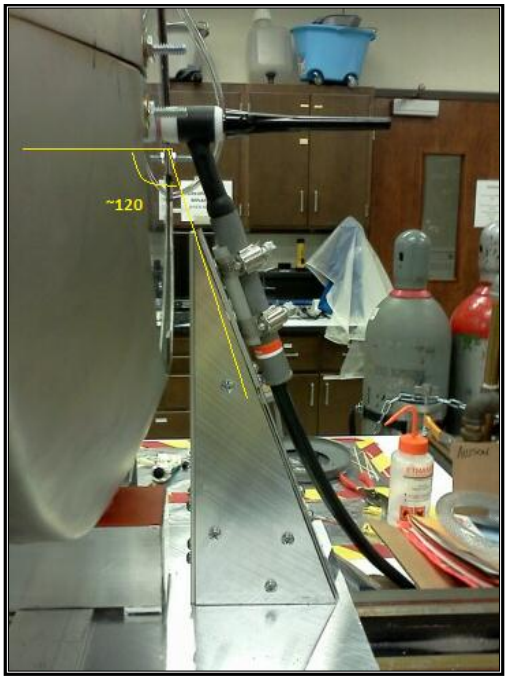

Figure 3-34: The angle of the tungsten stinger relative to the torch head.

The welder current was controlled using a foot amp troll. The amp troll allows the user to send a fraction of the maximum current set on the welder by compressing the pedal. This is similar to driving a car - the more the user presses on the pedal, the more current is sent. The torch head has a ceramic sheath in which an argon cover gas is passed through to cover the welding surface with argon, preventing oxidation. This was well suited for the RES since an argon cover gas is already required in the catch pan.

3.10 Spindle Holder Structural Support

Structural supports were needed to raise the spindles to the operational height for the catch pan. The center of the spindles collets were lined up with the center of the catch pan. These supports also aligned the spindles with the lathe bed so the carriage moves directly towards or away from the spindles.

Two variables were of interest when designing the structure support for the spindle holder. The first was the width of the base, which was wide enough so that the heavy spindle holder cannot accidentally tip over. The spindle holder is approximately 200 lbs and sits 43.18 cm (17 in) above the countertop. In order to prevent it from accidentally tipping over, a 50.8 cm (20 in) base was chosen requiring 235 lb of force to push it over. The second variable needed to be considered is how far the spindle extends past the rear of the lathe bed. Section 3.7 determined that the lathe bed needed to be 114.3 cm (45 in) in length, but the closest bed that could be found was 99 cm (39 in). Therefore, the structural supports were extended 15.3 cm (6 in) past the end of the lathe bed, and an adapter plate was aligned to the spindle holder with the lathe bed. The

structural supports were made out of construction grade 0.64 cm (0.25 in) thick aluminum channels and I-beams. The complete list of parts can be found in Appendix A.

4. PROCEDURE AND RESULTS

The procedures for running the RES and the procedures results from the first tests are summarized in this chapter. Section 4.1 summarizes the operation procedures used for the first tests. Section 4.2 summarizes the operation procedures used. Section 4.3 summarizes the results of the initial testing.

4.1 Operation Procedures

4.1.1 Alloy Pin Preperation

The metal undergoing atomization was first fabricated into a 0.954 cm (0.375 in) diameter pin starting from a 1.27 cm (0.5 in) diameter rod using a lathe machine. Aproximately 2.5 cm (1 in) of the rod was left at the original 1.27 cm (0.5 in) diameter to be inserted into the collet. The total length of the pin was kept under 12.7 cm (5 in), since the pin should not extend out of the collet more than ~10 cm (4 in) to minimize vibrational harmonics.

The 0.318 cm (0.125 in) – 0.794 cm (0.314 in) diameter tungsten electrode needed to be sharpened to a point before each operation in order to initiate the arc. Multiple electrodes were sharpened prior to operating the RES since a sharpened point is needed for each run. The electrodes were held in place by a clamp located on the torch head so that they can easily be interchanged between runs by loosening and tightening this clamp.

4.1.2 VFD Settings

In order to energize the VFD, the circuit breaker in the electrical enclosure box was closed by flipping it up, displaying the red bars. If the VFD doesn't power up, check the main breaker in the transformer. The remote keypad was then checked to ensure the VFD was in the "Stop" position by reading "---" on the display. If not, the red "Stop" button should be pressed on the remote keypad and startup paramaters should be verified. Using the remote keypad arrows, the frequency was increased to the operating level using Eq. 3-9 and left alone until the coolant is initiated.

4.1.3 Water, Air, and Argon Inititation

The water chiller was turned on and the flow rate was checked to ensure it was circulating around 2-3 gpm to the motorized spindle. The water lines were visually inspected to ensure there was no excessive leakage occuring. The air line valve was then opened and the air flow rate was checked to ensure air was being sent to the non-motorized spindle and slip ring cooling system. Finally, the argon line valve was opened ~0.125 of a radian and the flow rate was checked to ensure argon was flowing to the catch pan.

4.1.4 Welder Settings

The welder was wheeled into location and once the breaker on the welder was checked to be open, it was plugged in. The torch head and grounding clamp were connected and secured. The foot amp troll was then connected and placed in a

comfortable location. The breaker on the welder was then closed, which energizes the welder, and the current was set using a DC- polarity. Care was taken at this point to not press the foot amp troll as this would initiate the arc if the electrode was close enough to the pin about to be atomized. The electric circuit was then re-checked prior to operation to verify proper connections have been made.

4.1.5 Initiate RES

The catch pan was adjusted so that the tungsten stinger was aproximetaly 0.5 cm (1/5 in) from the pin about to be atomized by cranking the gear on the carriage. The green "Start" button on the remote keypad was then pressed initiating the motorized spindle. Once the spindle had ramped up to speed (defualt parameter takes 60s), the welding mask was placed on and the foot amp troll was compressed fully. After about 1s, the arc iniated. Once the pin began to melt, the puddle was radially propelled and the pin was consumed. As this happened, teh carriage was slowly cranked towards the pin to maintain the aproximetaly 0.5 cm gap. This continued until the catch pan came into contact with the spindle holder, at which time the foot amp troll was released and the red "Stop" button on the remote keypad was pressed. The spindle will then ramp down to a stop. The welder and VFD were then turned off by opening the breakers on the welder unit and in the elctrical enclosure. The argon line was then closed. The coolant was allowed to flow for five minutes per Dynomax’s recommendation before closing the air and water lines by closing the valves and turning off the water chiller.

4.2 Demonstration Test Description and Observations

The run in procedure recommended by Dynomax to ensure no damage occurred during transportation was first performed. The run in procedure checks for excessive friction in the bearings of the spindle. To do this, the motorized spindle was run at 10,000 RPM, 20,000 RPM, and 30,000 RPM for 30 minutes each. The temperature of the housing and bearings was monitored using a pyrometer. There was only a 2 °C temperature increase measured from the ends of the bearings at the highest RPM, well within the operating limitations. No run in procedure for the non-motorized spindle was mentioned in the installation documentation, but was performed at low RPM once the slip ring was installed by simply measuring the bearings after 10,000 RPM and 15,000 RPM.

The slip ring was installed along with one plate of the slip ring cooling system and the brushes. The system was run at 10,000 RPM for 10 minutes. The slip ring surface had no noticeable increase in temperature, and could be physically touched immediately after the operation ceased. This eased concern about the correlation for the Nusselt number and surface temperate of the slip ring during operation. The bearings of the non-motorized spindle as well as its housing were also monitored with no increase in temperature. This indicated that the cooling system may have been over designed and may not be necessary for system operation. The second plate was installed and the testing could commence.

The first attempt to atomize a 1.25 cm (0.5 in) diameter copper pin at 12,000 RPM failed due to the polarity used on the welder. During testing, 90A of DC+ melted

the tungsten electrode before the copper pin; DC- is required. Once DC- was used, a second attempt to atomize the pin failed because the current was too low. The third attempt was successful when the current was increased to 140A. The arc was needed for approximately 15s to produce 29g of copper powder. The fourth test atomized a 1 cm (0.4 in) copper pin rotating at 15,000 RPM using 100A. The fifth test was performed on the same copper pin rotating at 16,300 RPM using 120 A.

The first thing noticed after initiating the RES was the arc behavior. Once the arc is initiated, the tip of the sharpened tungsten electrode immediately melts, and the catch pan must slightly move towards the pin to compensate for the shortened electrode. If the arc is sustained through this, the pin will then began to immediately melt if the current is high enough, starting from the center of the pin outward. This lead to an unexpected facet of operation, the behavior of the molten metal at the tip of the rotating electrode.

As the tip of the pin began to melt, a "puddle" of molten copper would form. Almost as soon as it formed, centrifugal forces propelled the molten copper radially leaving a concave cavity, shown in Fig. 4-1. As this cavity grew, it caused the arc to jump from the center of the pin to the peripheral edge. As it jumped to the peripheral edge it would immediately melt it in a somewhat violent manner. To overcome this effect, a smaller diameter pin or a larger diameter tungsten electrode with higher current may be used. However, the larger diameter electrode would require a much more powerful welder so future tests may consider limiting the pin diameter to less than 0.95 cm (3/8 in).

Figure 4-1: The concave cavity formed during atomization of the Cu pin.

The last notable observation occurred during the microsphere collection phase. Approximately half of the microspheres fell into the drawer, while the other half stuck to the catch pan walls. In order to remove the copper microspheres, a brush was needed to sweep them off the walls. A higher flow rate on the argon jets at the top may help to alleviate any collection on the walls, and should be used even in the glove box.

4.3 Demonstration Test Product Characterization

The copper microspheres produced by the first RES run were collected, weighed, and then placed in the top of seven stacked sieves with decreasing mesh sizes. The top sieve used a 500 μm mesh, followed by a 250, 180, 125, 75, and 53 μm meshes. The

bottom sieve tray was a solid container. The stacked sieves were then clamped into place and vibrated using a Dual Manufacturing sieve shaker (model D-4326) shown in Fig. 4-2 for 15 minutes.

Figure 4-2: The Dual Manufacturing sieve used to filter the copper microspheres.

The contents of each sieve were then weighed to determine the fraction of microspheres in each size range. As expected, an increase in RPM reduced the median particle size. Figure 4-3 displays the results of the three tests.

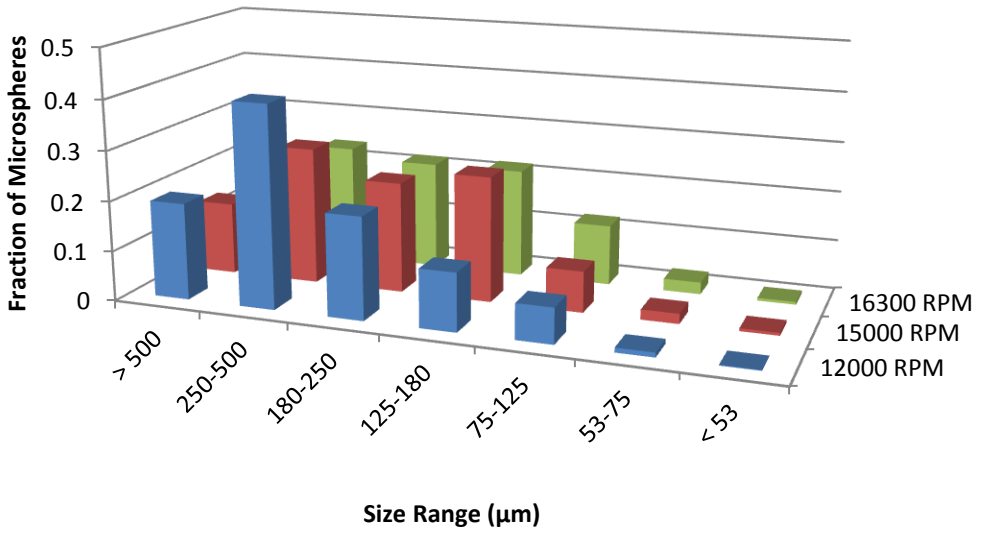

Figure 4-3: The size distribution of the Cu microspheres fabricated from the RES tests.

The general shape of the particles produced in each size range was determined using a Hirox digital microscope (model KH-1300). The 500 µm diameter and greater particles are shown in Fig. 4-4. The particles produced in this size range appear to have either coalesced during flight or when they hit the catch pan wall or perhaps they never fully separated from each other when propelled from the tip of the Cu electrode.

Figure 4-4: The Cu particles from the 500 μm mesh sieve tray.

The next size range was from the 250 μm mesh sieve tray. These particles are shown in Fig. 4-5. The particles in this size range appear to be partially forming into actual spheres and separating from each other. The irregular shapes are scarcer in this size range indicating more complete separation from the copper tip prior to solidification. However, the flatness of the microspheres indicates solidification did not occur fully prior to hitting the catch pan wall.

Figure 4-5: The Cu particles from the 250 µm mesh sieve tray.

The next size range analyzed is from the 180 µm mesh sieve tray. These particles were mostly spherical and are shown in Fig. 4-6. No irregular shapes were observed and only some were somewhat flat, indicating most of these micro-spheres solidified prior to hitting the catch pan wall.

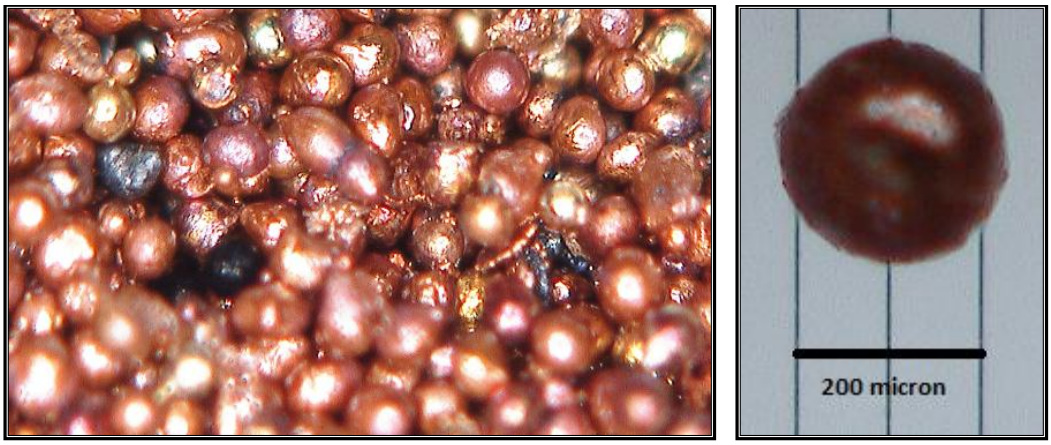

Figure 4-6: The Cu microspheres from the 180 µm sieve tray.

The remaining size ranges were all very similar in shape with strong sphericity, with only the particle diameter changing. Figures 4-7, 4-8, 4-9, and 4-10 show the microspheres from the 125 µm, 75 µm, 53 µm, and <53 µm mesh sieve trays, respectively.

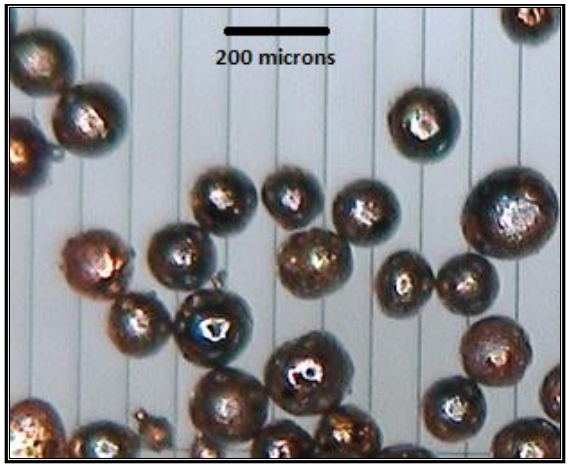

Figure 4-7: The Cu microspheres from the 125 µm sieve tray.

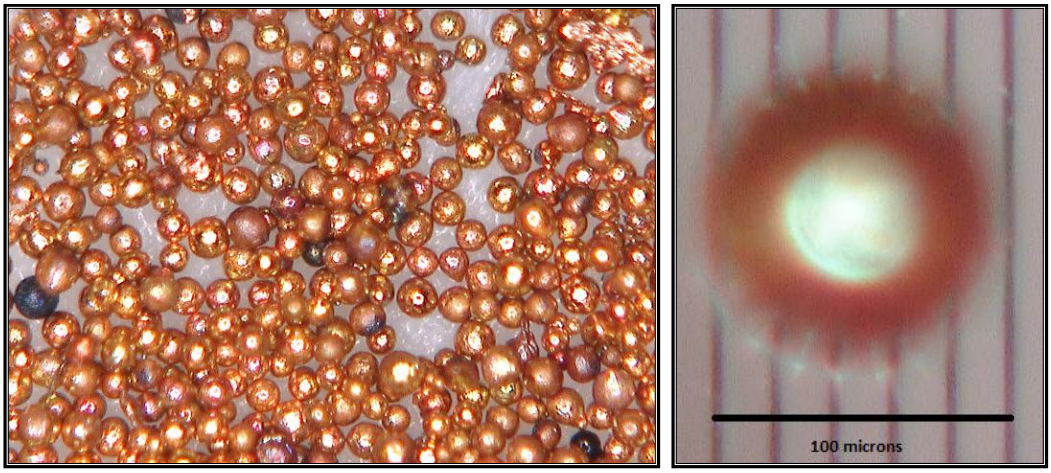

Figure 4-8: The Cu microspheres from the 75 µm sieve tray.

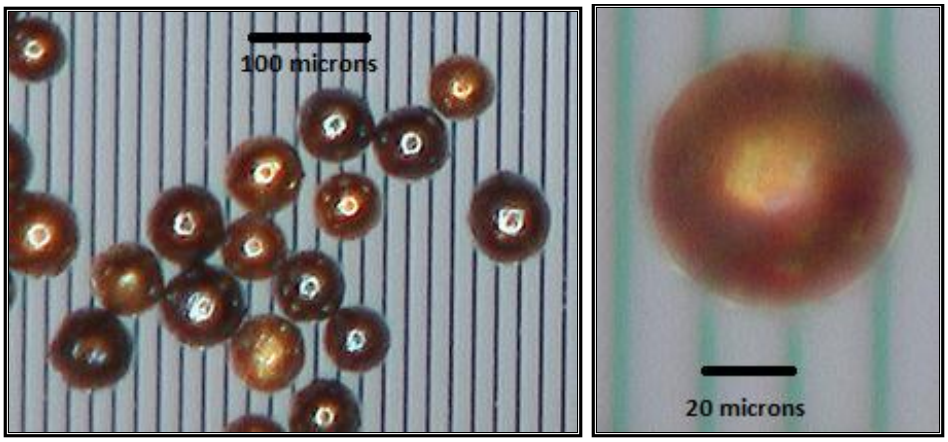

Figure 4-9: The Cu microspheres from the 53 μm sieve tray.

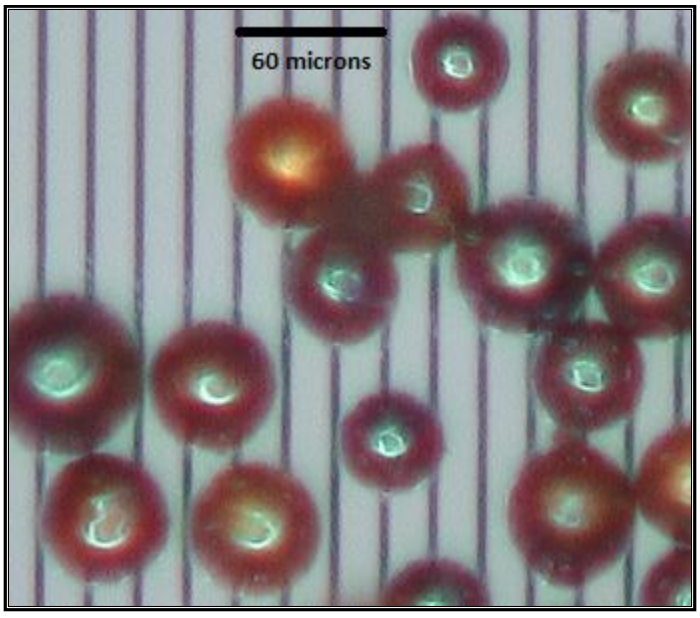

Figure 4-10: The Cu microspheres from the bottom sieve tray (<53 μm).

5. SUMMARY

The RES was designed based on the original REP by Starmet Incorporated and a similar system designed by INL for producing U-7Mo microspheres. The RES was designed to operate at rotation speeds up to 40,000 RPM while melting the tip of a 1.27 cm (0.5 in) diameter U-Zr pin using an electric arc passing up to 200 A. Every component of the system can be disassembled and passed through a 35.56 cm (14 in) diameter air lock of a glove box. The RES was assembled and tested on the benchtop in an air atmosphere using copper pins so that it could be optimized prior to moving into a glove box.

5.1 System Design

A horizontal orientation was chosen to allow for easier operation in a glove box and for powder to collect into a single drawer at the bottom of the catch pan. There were no perceived problems with operating the machine in a horizontal orientation and much of the powder did fall to the bottom of the catch pan and into a hole where it was collected by the drawer. However, there was some powder that "stuck" to the walls of the catch pan and required a wire brush to "sweep" it off. This may be challenging when the RES is transferred into the glovebox when the range of motion is restricted by the gloves. Perhaps a higher argon flow directed at the walls of the catch pan (discussed below) could prevent much of this powder from sticking.

5.1.1 Electrical Brushes, Holders, and the TIG Welder

Ten electrographitic brush contacts were assembled in their holders and attached to structural supports over the slip ring to allow electric contact to be made with the rotating slip ring. The ground of a Lincoln TIG 225 welder was connected to these holders while the torch head of the welder was held in place by structural supports that centered the torch head in the center of catch pan so that it was in line with the rotating electrode. The welder and brushes were designed to pass up to 200 A DC. The brushes were tested up to 140 A at 16,300 RPM with no noticeable problems or wear.

5.1.2 Spindles, Spindle Holder, and Slip Ring

The RES used two spindles that were held in a custom made holder that aligned the two. Two spindles were used so that a 5 cm (~2 in) diameter 303 stainless steel slip ring could be inserted into each of the 1.27 cm (0.5 in) EX-20 collets mounted on both of the spindles. This holder was then mounted to a retrofitted lathe bed so that a carriage could be utilized while feeding the catch pan into the pin as it was atomized. The motorized spindle was water cooled and capable of rotating up to 40,000 RPM with a torque of 0.44 N-m and controlled using a 2.5 hp VFD. The other spindle is air cooled and has electrically insulated bearings as well as 1.27 cm (0.5 in) EX-20 collets on both ends. The two spindle design did appear to alleviate vibrational harmonics resulting from imbalances within the slip ring. Although the slip ring was firmly held, the bearings of the spindle may still limit operation during those harmonics due to the weight of the stainless steel slip ring and could possibly pose to be a failure mechanism. A lighter slip

ring would alleviate the forces exerted on the bearings by the slip ring during those harmonics.

5.1.3 Catch Pan, Drawer, and Carriage

The catch pan was a pseudo cylinder mounted on the carriage of a retrofitted lathe machine. It was mounted in a vertical orientation and had a hole at the bottom in which the powder produced could fall into a drawer for easy removal. Argon spray nozzles were installed on the inside top wall to direct argon on the side walls to alleviate oxidation while being tested in an air environment. As discussed above, much of the powder "stuck" to these walls which required a metal brush to "sweep" of. The drawer at the bottom worked well for anything that fell through the hole. Although the argon spray nozzles were installed to alleviate oxidation, they could serve to force powder into the hole if a large increase in argon flow could be achieved.

Two inserts were installed on each end of the catch pan. The insert nearest to the spindles was made out of aluminum sheet metal and had a 10 cm hole to allow the pin to enter when the catch pan was fed into the pin being atomized. The insert nearest to the operator was made out a high temperature polymer and had a 2 cm hole for the torch head to enter and allowed the operator to see the arc during operation so that the distance between the pin being atomized and the tungsten electrode, held in place by the TIG torch head, could be adjusted. The aluminum sheet metal insert was scarred from the molten spray and steel may be a better choice. The high temperature polymer insert worked well with no problems of scarring noticed.

5.2 Recommended Future Work

The operating parameters for the characterization of U-xZr need to be carefully planned out. First, the RPM of the RES should start slow and build up as data is collected. The reason for this is because replacing the motorized spindle and/or brushes is not only expensive, but takes months to get replacement parts. Second, another slip ring should be considered after the RES is transferred into the glove box. The slip ring may perform differently in an argon environment and a lighter weight will reduce force on spindle bearings. Lastly, a quality assurance plan should be finalized.

5.3 Proposed RES Quality Assurance Plan

The quality assurance plan for the RES ensures that the operating parameters used for each test are known, accurate, and replicable. The key parameters that must be recorded for test reproducibility are RPM, pin diameter, pin length extending from the collet, and current used to melt the pin. The minor paremeters that must be recorded for system reproducibility are the air, argon, and water flow rates for the cooling system.

5.3.1 Verification of RPM

A non-contact tachometer can verify the RPM displayed by the VFD. The non-contact tachometer displayed in Fig. 5-1 comes with a NIST certificate and can be found at McMaster Carr. An optical tape is placed on the flat area of the spindle shaft near the collet and an optical sensor on the tachometer measures the revolutions over time, shown in Fig. 5-2.

Figure 5-1: The NIST certified non-contact tachometer [23].

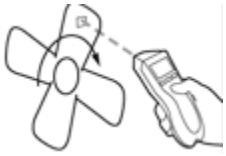

Figure 5-2: Illustration of how a non-contact tachometer works [23].

5.3.2 Verification of Current

The current required to melt a specific alloy and pin size can be determined by measuring the voltage drop across an in-line shunt. A shunt, like the one pictured in Fig. 5-3, has a know resistance and can be easily connected to a volt meter while the welder operates. The current can then be determined by the voltage drop measured using

$$I = \frac{V}{R} \tag{5-1}$$

where V is the measured voltage drop and R is the known resistance.

Figure 5-3: A shunt used to determine the current of the welder [24].

5.3.3 Quality Assurance Procedure

A reference pin can be used to determine the loaded RPM and current required to melt a specific alloy. This reference pin will be a part of a batch of identical pins fabricated. Prior to inserting this reference pin, an in-line shunt will be connected to the ground circuit of the welder, and the welder current set to maximum capacity. The first pin will be inserted into the collet and brought up to the operating RPM and verified using a non-contact tachometer, both will be recorded. An assistant mau be necessary to measure the RPM with the non-contact tachometer. The operator will then compress the foot amp troll until melting begins and will verbally relay it to the assitant who will then measure and record the voltage drop across the shunt. This voltage drop can then be correlated to the current using Eq. 5-1 Lastly, the air, argon, and water flow rates will be recorded using in-line flow meters.

REFERENCES

1. Taiwo, T.A. and Kim, T.K., 2010, "Fuel Cycle Analysis of Once-through Nuclear Systems," ANL-FCRD-308, Argonne National Laboratory, Argonne, IL.
2. Ahlfeld, C., Gilleland, J., Weaver, K.D., Whitmer, C., and Zimmerman, G., 2010, "A Once-Through Fuel Cycle for Fast Reactors," Journal of Engineering for Gas Turbines and Power, **132**(10), pp. 102917-1 – 102917-6.
3. Walters, L., 1999, "Thirty Years of Fuels and Materials Information from EBR-II," Journal of Nuclear Materials, **270**(1-2), pp. 39-48.
4. Clark, C.R., Fielding, R.S., Hallinan, N.P., and Knighton, G.C., 2010, "INL Laboratory Scale Atomizer," INL/EXT-10-17574, Idaho National Laboratory, Idaho Falls, ID.
5. Kaufman, A. R., 1963, "Method and Apparatus for Making Powder," U.S. Patent 3,099,041.
6. German, R., 1994, "Powder Metallurgy Science," 2nd ed., Metal Powder Industries Federation, Princeton, NJ.
7. McDeavitt, S.M. and Solomon, A.A., 1996, "Hot-isostatic Pressing of U-10Zr by a Coupled Grain Boundary Diffusion and Creep Cavitation Mechanism," Journal of Nuclear Materials, **228**(2), pp. 184-200.
8. Miller, S.A. and Roberts, P.R., 1998, "The Rotating Electrode Process," ASM Handbook, **7**, pp. 97-101.
9. DeMita, H.J. and Miller, S.A., 1999, "System and Method for Producing Fine Metallic and Ceramic Powders," U. S. Patent, 5,855,642.

10. Clark, C.R., Jue, J.F., and Muntifering, B.R., 2007, "Production and Characterization of Atomized U-Mo Powder by the Rotating Electrode Process," INL/CON-07-13156, Idaho National Laboratory, Idaho Falls, ID.
11. Roberts, P.R., 1986, "Powders Made by the Rotating Electrode Process," Starmet International Report.
12. Clark, C. R., 2010, Nuclear Programs Directorate, Idaho National Laboratories, private communication.
13. Mersen U.S.A., n. d., "Brushes for Electrical Machines Technical Guide," from http://www.mersen.com/uploads/tx_mersen/514_3-brushes-for-electrical-machines-en.pdf.
14. Patel, A., 2011, Applications Engineer, Mersen U.S.A., private communication.
15. Bohn, M.S., Kreith, F., and Manglik, R.M., 2010, "Principles of Heat Transfer," 7th ed., Brooks/Cole, Pacific Grove, CA.
16. MTI Corporation, 2010, "Material Safety Data Sheet for Conductive Graphite Powder," from http://www.mtixtl.com/MSDS/Conductive%20Graphite%20Powder.pdf.
17. AT Precision, n. d., "Stainless Steel Machining Services," from http://www.atprecision.com/machining/materials/stainless-steel-machining.shtml.
18. Little, G.M., 1931, "The Application of the Helical Groove to Slip Rings and Commutators," Journal of American Institute of Electrical Engineers, **50**(2), pp. 718-722.

19. McMaster-Carr, n. d., “Flat Spray Nozzles,” from http://www.mcmaster.com/#spray-tips/=i1pszu.

20. Popoli, W., 1998, “High Speed Spindle Design and Construction,” from http://www.mmsonline.com/articles/high-speed-spindle-design-and-construction.

21. Lenze AC Tech, n. d., “SCF Series Installation and Operation Manual,” SFO1U.

22. Lincoln Electric, 2007, “Precision TIG 225 Operators Manual,” IM895.

23. McMaster-Carr, n. d., “Noncontact Tachometers,” from http://www.mcmaster.com/#tachometers/=i1prui.

24. Gander MTN., n. d., “Blue Sea DC Current Shunt 200A/50mV Analog,” from http://www.gandermountain.com/modperl/product/details.cgi?pdesc=Blue-Sea-DC-Current-Shunt-200A/50mV-Analog&i=85678&r=view&aID=506Y6&cvsfa=2586&cvsfe=2&cvsfhu=3835363738&s_kwcid=goobasecontent_goobasecontent_filler&cID=GSHOP_85678.

APPENDIX A

PARTS

GRADE GROUP	GRADE	Apparent density	Resistivity µΩ.cm µΩ.inch	Shore Hardness	Flexural strength MPa PSI	Contact drop ΔU en V	Friction	Maximum current density A/cm² A/inch²	Upper speed limit m/sec. ft/sec.	Metal content %
Carbo-graphitic	A 121	1,75	2 200 (710)	30	25	M	L	12 to 20 (75 to 125)	≤ 15 (≤ 49)	
	A 122	1,67	45 000 (16 000)	27	20	H	L	10 to 12 (65 to 75)	≤ 15 (≤ 49)	
	A 176	1,60	52 500 (21 717)	40	20	H	L	8 to 10 (50 to 65)	30 (98)	
	A 210	1,57	25 000 (10 000)	30	16	M	L	8 to 10 (50 to 65)	≤ 25 (≤ 82)	
	A 252	1,57	45 000 (16 706)	27	16	H	L	10 to 12 (65 to 75)	≤ 25 (≤ 82)	
Soft graphitic	LFC 501	1,46	1 900 (838)		8	M	M	6 to 10 (40 to 65)	75 (246)	
	LFC 554	1,26	2 000 (838)		10	M	M	11 to 13 (71 to 84)	90 (295)	
Electro-graphitic	EG 34D	1,60	1 100 (463)	35	25	M	M	12 (75)	50 (164)	
	EG 389P	1,49	1 600 (668)	29	19	M	M	12 (75)	50 (164)	
	EG 396	1,52	1 600 (668)	27	19	M	M	12 (75)	50 (164)	
	EG 362	1,62	2 500 (1 045)	35	21	M	M	12 (75)	50 (164)	
	EG 40P	1,62	3 200 (1 336)	57	27	M	M	12 (75)	50 (164)	
	EG 313	1,70	4 700 (1 963)	54	21	M	L	12 (75)	50 (164)	
	EG 367	1,53	4 100 (1 720)	48	21	M	M	12 (75)	50 (164)	
	EG 332	1,52	4 200 (2 025)	48	21	M	M	12 (75)	50 (164)	
	EG 387	1,63	3 300 (2 000)	60	39	M	M	12 (75)	50 (164)	
	EG 300	1,57	4 200 (1 680)	58	24	M	L/M	12 (75)	50 (164)	
	EG 98	1,60	3 400 (1 503)	60	33	M	M	12 (75)	50 (164)	
	EG 369	1,57	5 100 (2 030)	55	25	M	M	12 (75)	50 (164)	
	EG 319P	1,46	7 200 (3 007)	52	26	H	M	12 (75)	50 (164)	
	EG 321	1,46	6 600 (1 420)	54	26	H	M	12 (75)	50 (164)	
	EG 365	1,62	5 300 (2 840)	48	15	M	M	12 (75)	50 (164)	
Impregnated electro-graphitic	EG 7099	1,72	1 150 (463)	40	34	M	M	12 (75)	45 (148)	
	EG 9599	1,61	1 600 (640)	33	28	M	M	12 (75)	45 (148)	
	EG 9117	1,69	3 300 (1 320)	77	32	M	M	12 (75)	50 (164)	
	EG 8019	1,77	4 700 (1 880)	77	31	M	M	12 (75)	45 (148)	
	EG 8067	1,67	3 900 (1 600)	77	36	M	M	12 (75)	45 (148)	
	EG 8220	1,82	5 000 (2 180)	90	48	M	M	12 (75)	50 (164)	
	EG 7097	1,68	4 000 (1 560)	80	35	M	M	12 (75)	50 (164)	
	EG 341	1,57	7 025 (2 800)	74	34	H	M	12 (75)	50 (164)	
	EG 364	1,58	6 500 (2 720)	73	35	H	M	12 (75)	50 (164)	
	EG 6489	1,57	6 900 (2 720)	75	35	H	M	12 (75)	50 (164)	

Figure A-1: A tabulated list of various brushes offered by Mersen [13].

GRADE GROUP	GRADE	Apparent density	Resistivity µΩ.cm µΩ.inch	Shore Hardness	Flexural strength MPa PSI	Contact drop ΔU en V	Friction	Maximum current density A/cm² A/inch²	Upper speed limit m/sec ft/sec	Metal content %
Bakelite graphite	BG 412	1,82	14 000 (4 400)		36	H	M	8 to 10 (51 to 77)	35 (115)	
	BG 469	1,80	10 000 (4 000)		34	H	M	6 to 8 (77)	35 (115)	
	BG 400	1,50	25 000 (9 500)		25	H	M	8 to 10 (51 to 77)	40 (131)	
1- Agglomerated	C 6958	2,50	350 (44)		30	VL	M	10 to 25 (130 to 220)	≤ 32 (98)	25
	CG 33	2,30	500 (200)		27	VL/L	L	10 to 12 (65 to 75)	40 (131)	30
Metal graphite	C 8386	2,80	100 (44)		29	VL	L/M	20 to 30 (130 to 220)	≤ 30 (98)	46
	CG 651	2,95	130 (55)		30	VL	L	12 to 14 (75 to 90)	35 (115)	49
	CG 665	4,05	30 (12)		50	VL	L	15 to 20 (100 to 130)	30 (98)	65
	CG 75	4,65	12 (4)			VVL	L	16 (105)	25 (82)	77
	OMC	6,00	7 (2)		77	VVL	L	25 to 30 (160 to 200)	20 (66)	90
	MC 79P	5,20	7 (3)		98	VVL	L/M	25 to 30 (160 to 200)	20 (66)	83
	MC 12	6,00	32 (14)		173	VVL	L/M	25 to 30 (160 to 200)	20 (66)	91
	MC 689	5,95	23 (10)		138	VVL	L/M	25 to 30 (160 to 200)	20 (66)	89
2- Metal impregnated	M 609 (4)	2,00	450 (175)	35	38	VL/VVL	VVL	12 to 15 (75 to 100)	35 (115)	45
	M 673 (4)	1,72	1 100 (430)	35	26	VVL	H	10 to 12 (65 to 75)	40 (131)	5,5
	M 9426	1,62	1 775	24	16	VVL	M	12 to 15 (75 to 100)	45 (131)	9
	M 621	3,00	500 (200)	34	39	VVL	M	40 (267)	40 (131)	44
	M 9020	1,75	2 700 (200)	68	37	L		12 to 15 (75 to 100)	45 (131)	5
	M 8295	1,80	1 775 (200)	54	34	VVL	M	12 to 15 (75 to 100)	45 (131)	9

Figure A-2: A continued tabulated list of various brushes offered by Mersen [13].

Table A-1: The parts required to assemble the carriage for the RES.

Part #	Description
P0516501	Hand Wheel
P0516114	Oil Cup 6mm
Pk69M	Key 4 x 4 x 12
P0516504	Round Nut 26 x 12 x 8
PS12M	Philip Head Screw M3-.5 x 6
P0516506	Oil-Stopping Felt
PS31M	Philip Head Screw M6-1 x 35
P0516508	Saddle Leadscrew
P0516509	Saddle
PS02M	Philip Head Screw M4-.7 x 12
P0516511	Clearance Nut 23 x 31 x 14
PS50M	Philip Head Screw M3-.5 x 12
PN06M	Hex Nut M5-.8
P0516514	Dog Point Set Screw M5 x 25
P0516515	Pad Iron Gib
P0516516	Cross Slide
PS09M	Philip Head Screw SCR M5-.8 x 10
P0516518	Cross Slide Spacer
PS39M	Philip Head Screw M8 -1.25 x 10
P0516520	Gib Strip
P0516521	Rear-Clamp Plate
PS56M	Philip Head Screw SCR M4-.7 x 16
PS40M	Philip Head Screw M5-.8 x 16
PN04M	Hex Nut M4-.7
PS04M	Philip Head Screw M8-1.25 x 20
PS06M	Philip Head Screw M5-.8 x 20
P0516527	Oil-Stopping Felt
P0516528	Protecting Panel
P0516529	Protecting Panel
P0516530	Front-Clamp Plate
P0516531	Braking Plate
P0516532	Leadscrew Support
PW03M	Flat Washer 6mm
P0516534	Handle Bolt 60.5 x 10 x 8
PB08M	Hex Bolt M6-1 x 20
P0516536	Handle Sleeve

P8101	Thrust Bearing 8101
P0516538	Spring Plate
P0516539	Index Ring
PRP58M	Roll Pin 6 x 45

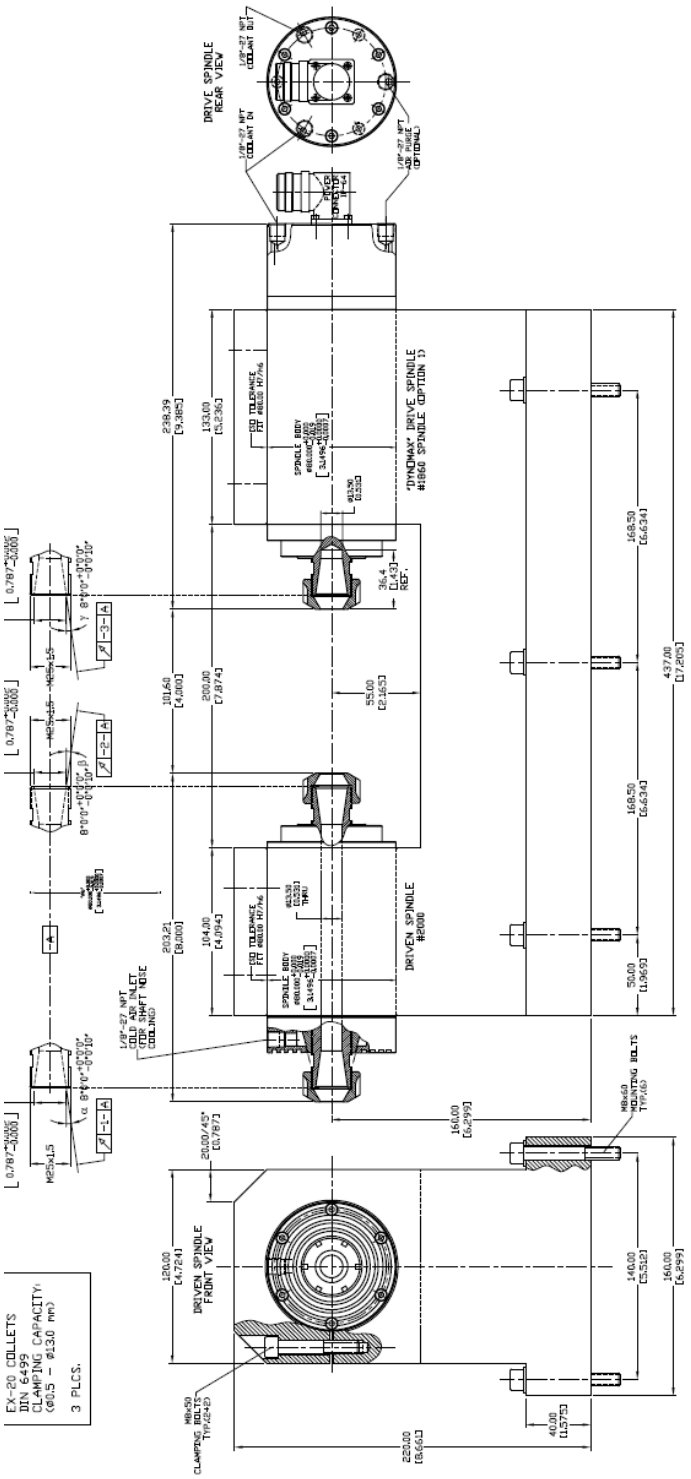

Figure A-3: The engineering drawing for the two spindles and their holder.

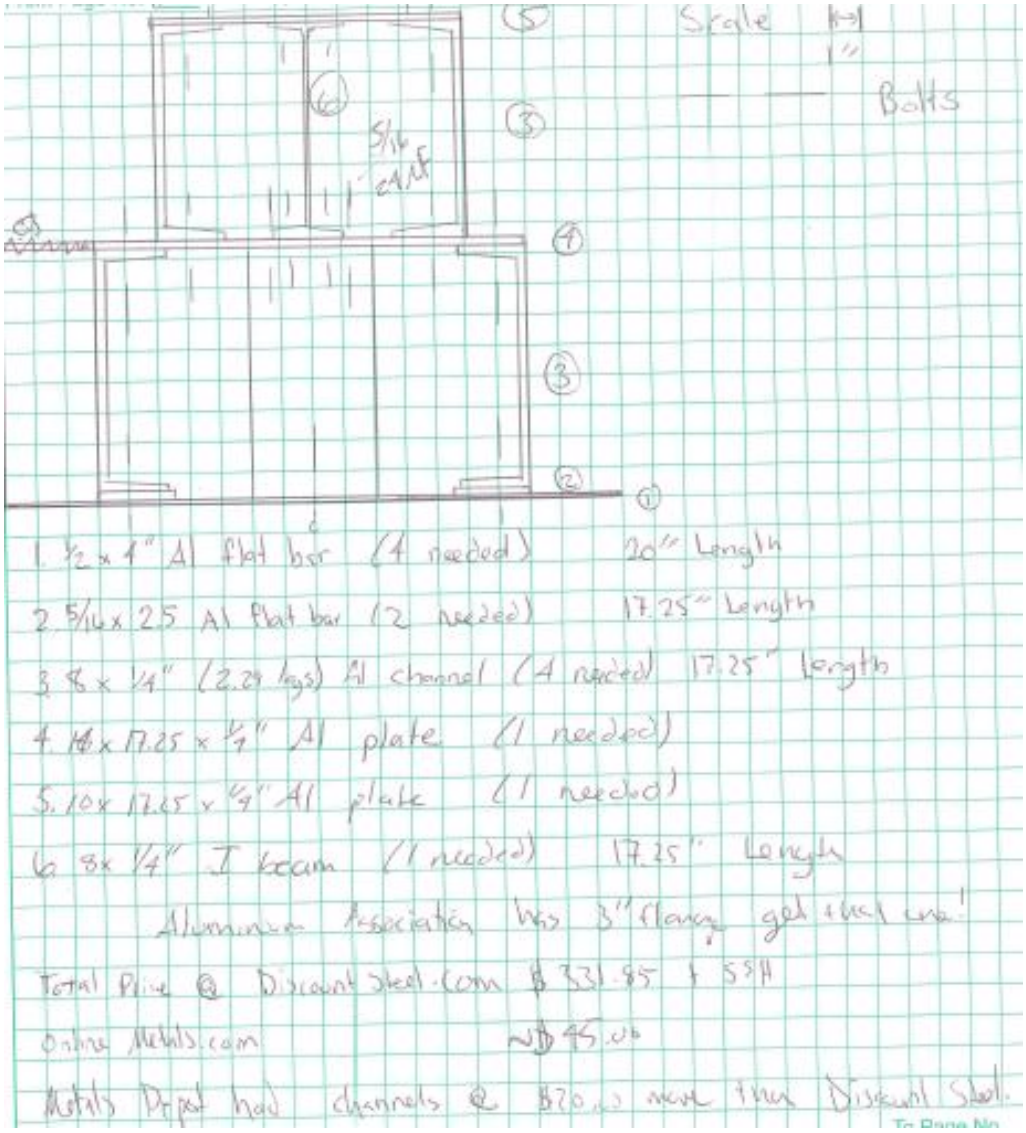

Figure A-4: The list of parts used for the structural supports.

APPENDIX B

PROCEDURES

1. The procedure for making the slip ring.

   Begin with a 2.125 in diameter 303 stainless steel cylinder around 10 in long.

   1.1 Insert the cylinder into a metal lathe and drill the tail stock centering hole so the tail stock can support the cylinder when turning it down.

   1.2 Insert the tail stock and lock it into place.

   1.3 Turn down a 6 in long section beginning at the end supported by the tails stock to 2 in, 0.01 in at a time around 400 RPM.

   1.4 Measure 5 in from the near the tail stock and mark.

   1.5 Adjust the feed rate to 4 threads per inch. Using the cross feed, move the cutting bit in 0.015” at the end near the tail stock and engage automatic feed. As soon as the bit begins to cut the mark in the previous step, disengage the automatic feed or damage will occur.

   1.6 Adjust the speed to around 1500 RPM and polish the cylinder starting with 250 grit sandpaper followed by 350, 450, and 500 grit.

   1.7 Measure and mark the center of the 6 in long section at 2 in diameter.

   1.8 Using a plunge bit, plunge into the slip ring at the following locations until the diameter is 0.75 in:

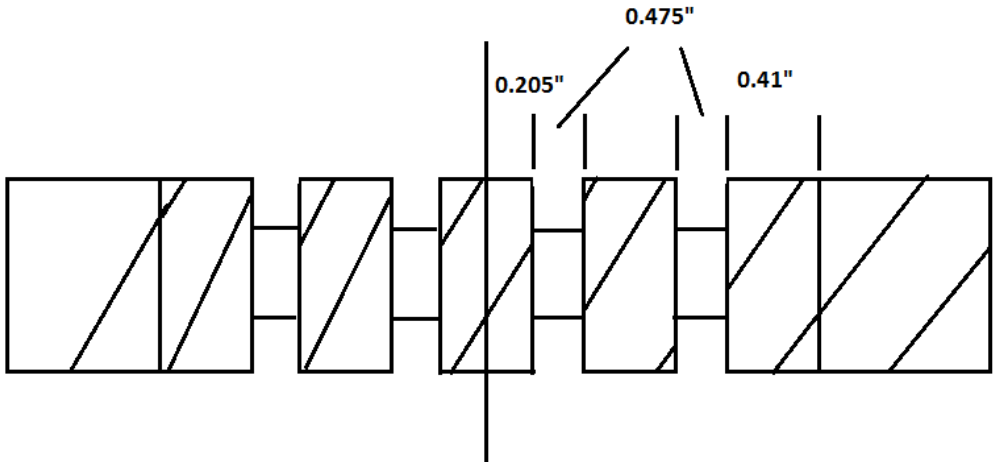

1.9 On the end near the tail stock, plunge down to 0.5 in followed by the opposite end.

1.10 Using a cutting bit, cut through the cylinder at 2.75 in from the center towards the tail stock followed by 2.75 in from the center away from the tail stock.

2. The procedure for making the catch pan.

1st Step: Cut a hole in the plates

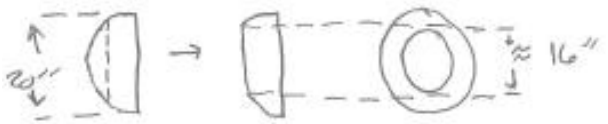

I would like the depth of each to be 3", so a second cut may be necessary

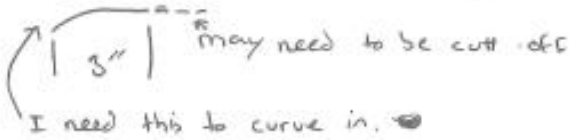

2nd Step: Weld the two plates together

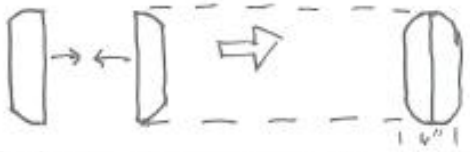

3rd Step: Cut (horizontally) the welded piece in half

4th Step: Fill the inside seam with filler and grind smooth (As best as you can)

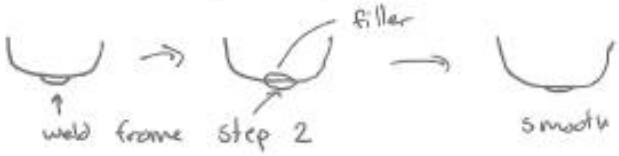

⚠ This may not be necessary if weld penetrated all the way through

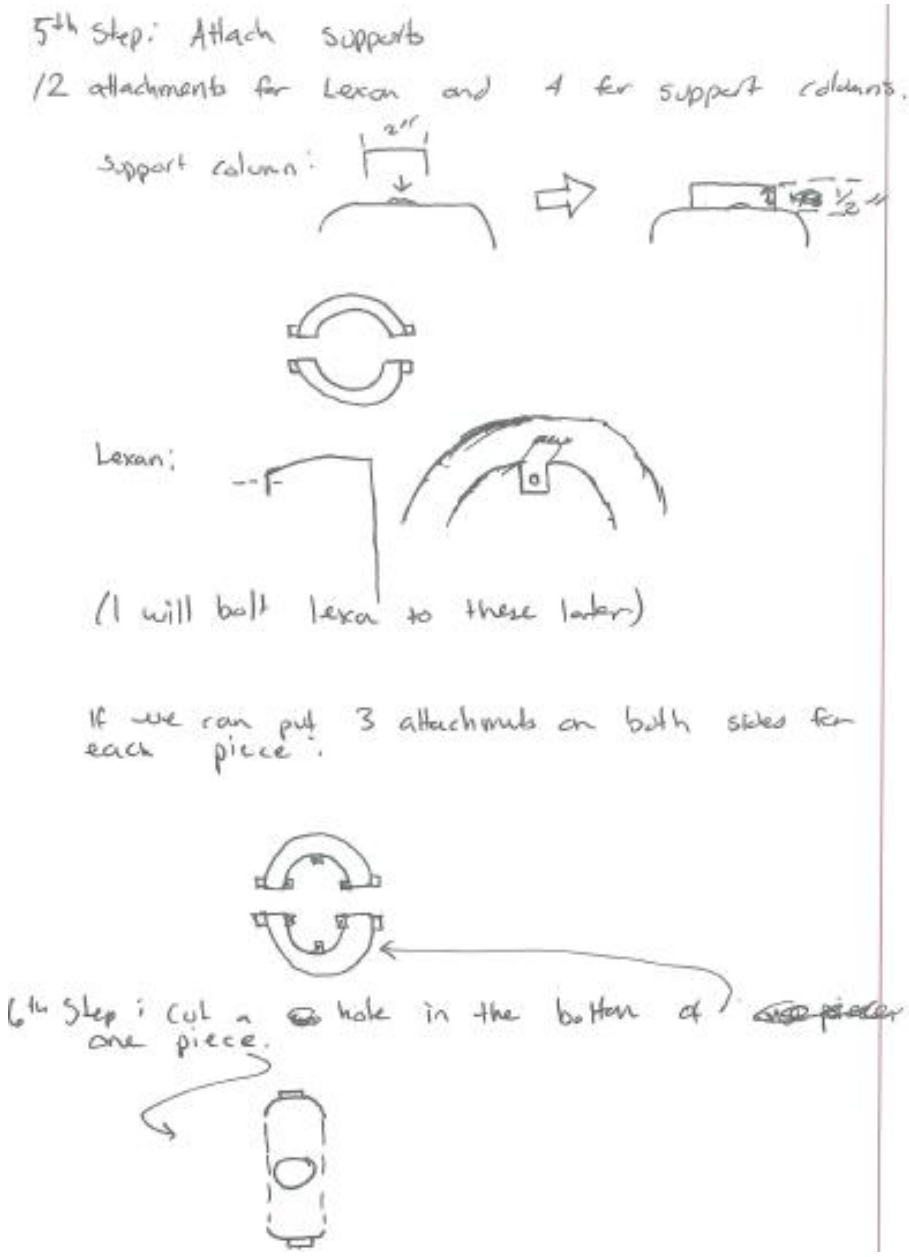

Figure B-2: The instructions given to Byran Custom Fabricators for fabricating the catch pan.

APPENDIX C

VFD PROGRAMMING

Parameter Number	Parameter Name	Factory Defualt	RES Setting
1	Line Voltage	High (01)	High (01)
2	Carrier Frequency	6 kHz (02)	8Hz (03)
3	Start Method	Normal (01)	Normal (01)
4	Stop Method	Coast (01)	Ramp (03)
5	Standard Speed Source	Keypad (01)	Keypad (01)
14	Control	Terminal Strip (01)	Remote Keypad (02)
15	Serial Link	With Timer (02)	With Timer (02)
16	Units Editing	Whole Units (02)	Whole Units (02)
17	Rotating	Forward Only (01)	Forward and Reverse (02)
19	Acceleration Time	20	40
20	Deceleration Time	20	60
21	DC Brake Time	0	0
22	DC Brake Voltage	0	0
23	Minimum Frequency	0	0
24	Maximum Frequency	60	667
25	Current Limit	180%	180%
26	Motor Overload	100%	100%
27	Base Frequency	60Hz	667Hz
28	Fixed Boost	1%	1%
29	Accel Boost	0%	0%
30	Slip Compensation	0%	0%
36	Skip Speed	0Hz	367Hz
38	Skip Bandwidth	0Hz	50Hz
39	Speed Scaling	0	0
40	Frequency Scaling	60	60
41	Load Scaling	200%	200%
42	Accel/Decel #2	20s	20s
43	Serial Address	1	1
44	Password	225	120